2014

Design Simulation for Solar Energy Research and Education

Samuel J. Schlitzer
Bucknell University, sjs057@bucknell.edu

Design Simulation for Solar Energy Research and Education

by

Samuel J. Schlitzer

A Thesis Submitted to the Honors Council

For Honors in Mechanical Engineering

5/08/14

Approved by:

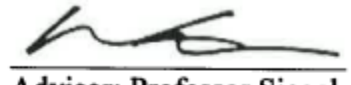

Advisor: Professor Siegel

Department Chairperson: Professor Knisely

Acknowledgments

I would like to express my gratitude to my project advisor, Professor Siegel. The completion of this thesis would not have been possible without his knowledge and patience through this entire process. The advice and support Professor Siegel has provided not only during this thesis, but also in class as well as previous research has been invaluable. I would also like to thank the other members of my thesis committee, Professor Brahma and Professor Salyards, for their help to improve my work.

I would like to thank Professor Knisely for teaching me the importance of writing in engineering, as well as all of his guidance over the past four years.

I cannot thank Tyler Moore, Hugo McMenamin, and Hunter McGrogan enough for the time they volunteered to peer edit this report throughout the writing process. I would also like to thank the rest of my classmates and friends for their help and encouragement.

Last and certainly not least, I would like to thank my parents for their love and support.

Table of Contents

List of Tables

List of Figures

Abstract

Solar research is primarily conducted in regions with consistent sunlight, severely limiting research opportunities in many areas. Unfortunately, the unreliable weather in Lewisburg, PA, can prove difficult for such testing to be conducted. As such, a solar simulator was developed for educational purposes for the Mechanical Engineering department at Bucknell University. The objective of this work was to first develop a geometric model to evaluate a one sun solar simulator. This was intended to provide a simplified model that could be used without the necessity of expensive software. This model was originally intended to be validated experimentally, but instead was done using a proven ray tracing program, TracePro. Analyses with the geometrical model and TracePro demonstrated the influence the geometrical properties had results, specifically the reflector (aperture) diameter and the rim angle. Subsequently, the two were approaches were consistent with one another for aperture diameters 0.5 m and larger, and for rim angles larger than 45°.

The constructed prototype, that is currently untested, was designed from information provided by the geometric model, includes a metal halide lamp with a 9.5 mm arc diameter and parabolic reflector with an aperture diameter of 0.631 meters. The maximum angular divergence from the geometrical model was predicted to be 30 mRadians. The average angular divergence in TraceProof the system was 19.5 mRadians, compared to the sun's divergence of 9.2 mRadians. Flux mapping in TracePro showed an intensity of 1000 W/m^2 over the target plane located 40 meters from the lamp. The error between spectrum of the metal halide lamp and the solar spectrum was 10.9%, which was found by comparing their respective Plank radiation distributions. The project did not satisfy the original goal of matching the angular divergence of

sunlight, although the system could still to be used for optical testing. The geometric model indicated performance in this area could be improved by increasing the diameter of the reflector, as well as decreasing the source diameter. Although ray tracing software provides more information to analyze the simulator system, the geometrical model is adequate to provide enough information to design a system.

Introduction

Solar energy is a readily available power generation option in many parts of the world. As with all technologies, research and development are required to make cost effective and more efficient systems. Unfortunately, research is difficult in some regions due to weather limitations. It is important to still have an opportunity to test and demonstrate solar energy technologies to support research and development. A solar simulator is an apparatus that replicates the radiant energy of the sun using a lamp as the light source and a reflector to direct the resultant beam. It can be used for a multitude of industrial and educational purposes. The objective of this study is to develop a solar simulator that is capable of emulating the angular divergence, spectrum and intensity of natural sunlight. Such a simulator will enable solar energy-related teaching and research in regions like Lewisburg, PA, where inconsistent weather limits the opportunity to test solar energy systems using focusing optics.

The structure of a solar simulator can be broken into four basic components as shown in Figure 1. A power supply delivers electricity to the system's light source(s) (e.g. arc lamp), and a reflector is positioned to redirect the light from the lamp towards the target.

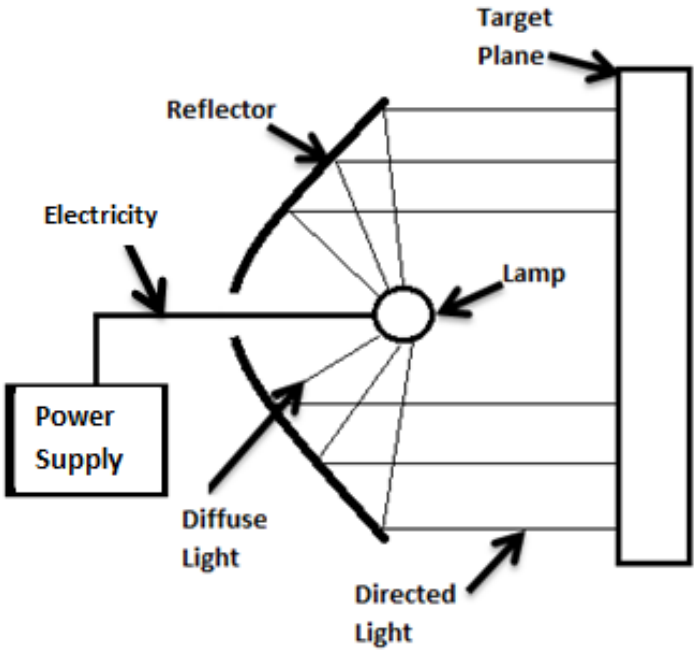

Figure 1: A diagram showing the basic form of a solar simulator

While Figure 1 shows a solar simulator in its simplest form, physical models can vary greatly. The three general configurations of solar simulators are used for 1) matching the spectrum and the intensity of the sun (e.g. Photovoltaic (PV) cell testing), 2) concentrating light (e.g. high flux production), and 3) collimating light (e.g. optical testing). There are relatively few options available to collimate light while matching the spectrum and intensity of natural sunlight and those that are readily available are expensive (10). A secondary objective of this study is to design a prototype to economically simulate sunlight while achieving an angular divergence better than current technology. The scientific deliverables for this project are shown in Table 1.

Table 1: Project deliverables

Criterion	Angular Divergence	Average Intensity at Target Plane	Spectral Distribution Diameter	Solar Spectrum	Efficiency[1] (%)	Cost
Target	9.2-25 mRadian	600-1000 W/m^2	0.9 meters	AM 1.5 Spectrum	40	Less than $3,000

The project began with the review of existing solar simulators. Conceptual design was started in parallel with the literature review, as other systems were evaluated to develop ideas for a new system. Two solar simulator concepts were subsequently investigated with one ultimately selected. A model was developed to efficiently assess the performance of a number of geometric configurations of the simulator concept. Following this, more detailed models were evaluated using a ray tracing program. The function of the ray tracing program, TracePro, was to validate lamp and reflector combinations that were ranked highly following earlier analysis with the simplified model, and to provide detailed output such as a flux map at the target plane.

Background

Most solar simulators fall into three categories, specifically spectrum/intensity matching, concentrating light, and collimating light systems. The first model replicates the solar spectrum and intensity and is primarily used for the testing PV cells (Figure 2).

[1] Defined as the ratio of the radiant power hitting the target plane to the radiant power emitted by the lamp

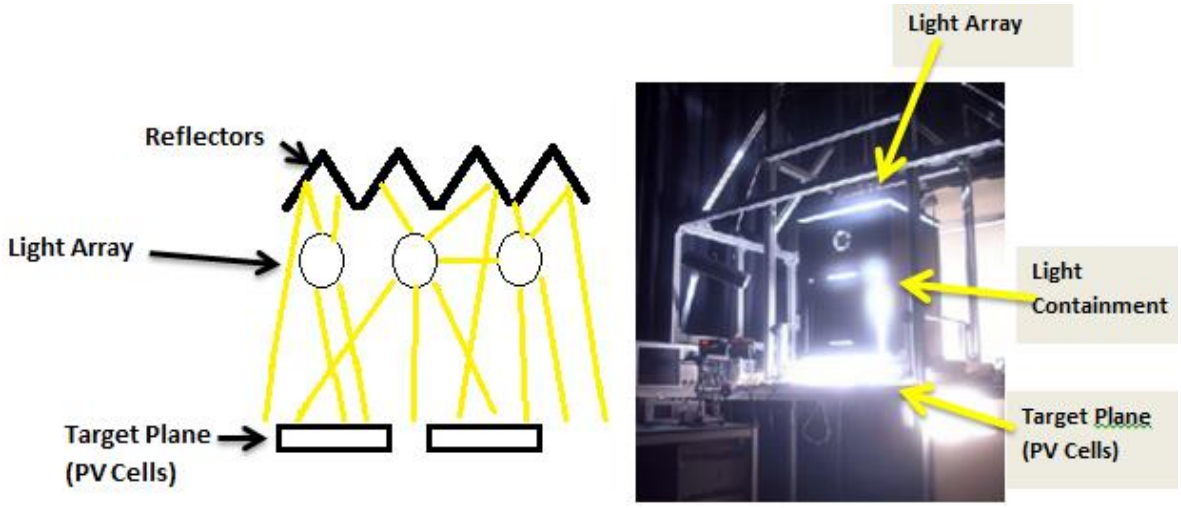

Figure 2: 2D rendering and physical version of a solar simulator used to test PV cells (1)

The spectrum/intensity matching systems typically do not collimate the light, as a collimated source is not required to measure the performance of PV cells. Instead, the systems' focus is to mimic the solar spectrum and emit an equivalent intensity to that of the sun that is uniformly distributed on the test plane. The solar spectrum is a range of wavelengths that contain radiant energy from the sun. The sun, approximated as a blackbody, has a surface temperature of 5800 K and releases a spectrum of light unique to that temperature (2). The energy content of sunlight varies continuously with wavelength, with a majority being in the visible spectrum, and is represented by AM 1.5 spectrum (2). The AM 1.5 spectrum shows the energy density from the sun as a function wavelength and includes the effects of the atmosphere on light reaching the surface of earth (Figure 3).

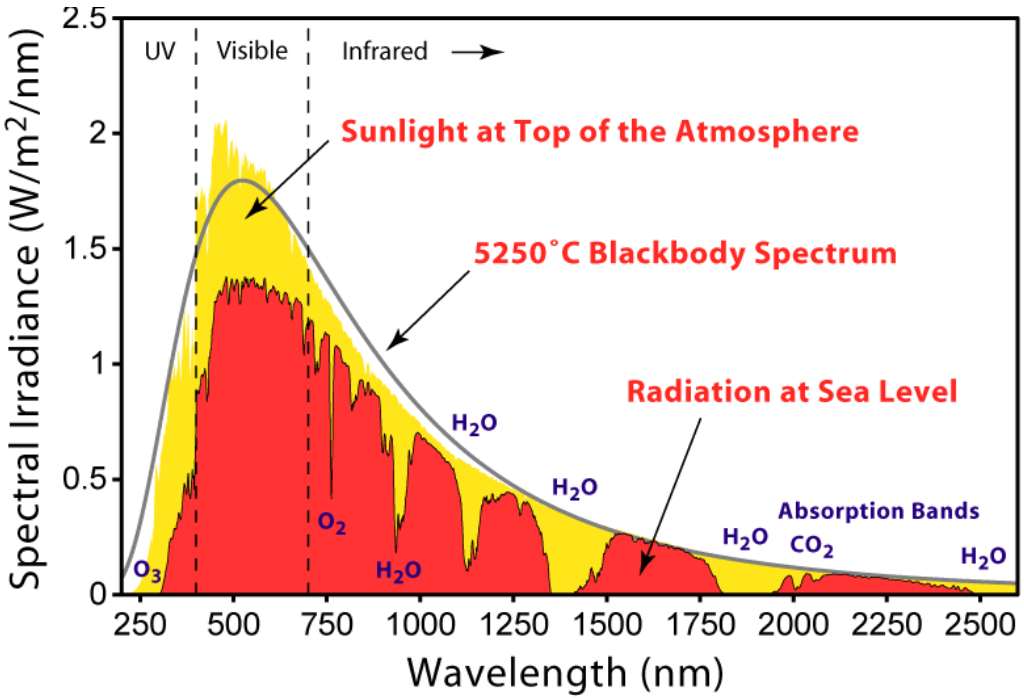

Figure 3: The AM 1.5 spectrum showing atmospheric absorption bands (4)

The power per unit area arriving at the Earth from the Sun defined as the intensity. The intensity of light on Earth can be calculated using the AM 1.5 Spectrum. The integral of the area under the solar spectrum curve (red portion) corresponds to the intensity of light on the surface of the Earth. A portion of the light incident on the atmosphere (the shaded yellow region) is filtered by water and carbon dioxide. The remaining light is incident on Earth's surface (the shaded red region). The intensity of AM 1.5 sunlight can be calculated by integrating the radiation at sea level for the wavelengths 250-3000 nm (Figure 4). This corresponds to approximately 1000 W/m^2 (4). In order to replicate the sun in a simulator, an artificial light source that has a spectral distribution approximating the solar spectrum is necessary, specifically the energy dense region of 400-1200 nm. Metal Halide arc lamps are typically used for this purpose.

Metal Halide lamps have a range of power outputs. The solar concentrator at Bucknell University is powered by a 1500 W Metal Halide lamp with a 7 mm source diameter. Lamps with larger power outputs typically have larger diameters. Most 2500 W Metal Halide lamps have a source size of 14 mm, although there is a commercially available 2500 W lamp with a 9.5 mm diameter. Power sources of this size would be capable of producing an intensity equivalent to the sun's while providing an accurate representation of the AM 1.5 spectrum (Figure 4).

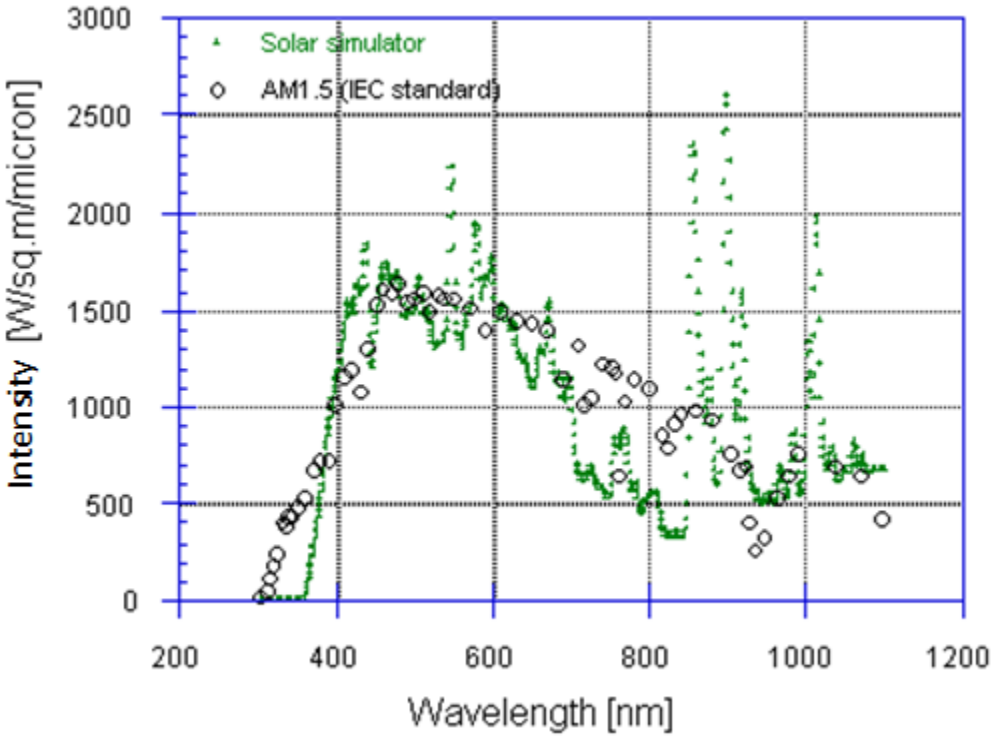

Figure 4: A comparison of the AM 1.5 Spectrum compared to a solar simulator with a metal halide arc lamp (6)

Figure 4 shows that the metal halide lamp's spectrum is a reasonable approximation of the solar spectrum, and is used in many simulators to test PV cells. Additionally, an equivalent distribution trend between the metal halide and AM 1.5 spectrum would produce a similar

intensity. While metal halide lamps are considered an acceptable approximation, research has been conducted to improve the accuracy of the lamps for use in applications more sensitive to the spectrum. Bazzi et al discusses another way to replicate the AM 1.5 spectrum with an array of LED lights (Figure 5) (**Error! Reference source not found.**).

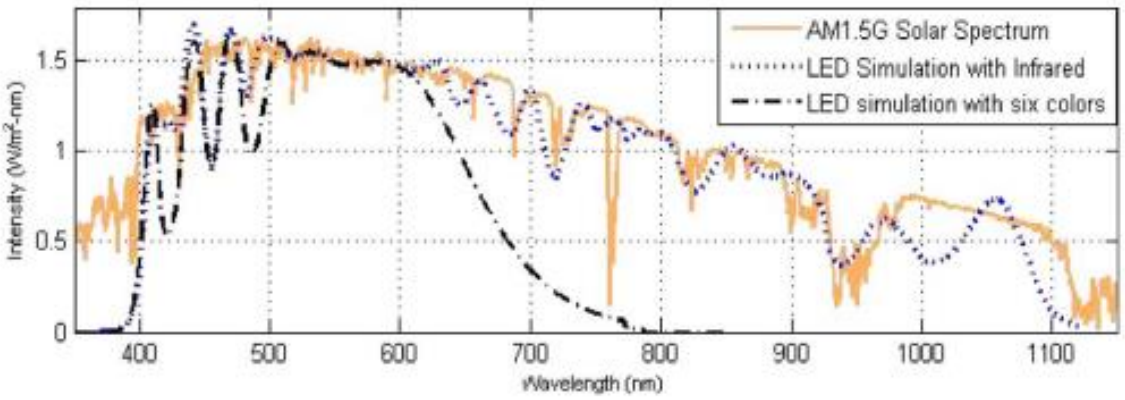

Figure 5: LED solar spectrum compared to the AM 1.5 solar spectrum (7)

Although the infrared LED array closely imitates the AM 1.5 solar spectrum, the accuracy comes with drawbacks. The LED lights that were used had low power requirements, and in the case of this experiment, only 17 Watts were transmitted onto the 0.005 m^2 target plane, which equates to an intensity 3400W/m^2 but would not meet the requirement to project over an area with a 0.9 meter diameter (**Error! Reference source not found.**). When tested, the array produced an ngular divergence of 192 mRadians. While this divergence does not hinder PV cell testing, it would not be suitable for testing optical equipment because light with a large angular divergence is extremely hard or impossible to refocus, making it impractical for optical studies.

Solar simulators can also be used to generate high temperatures through concentrating solar power (CSP) systems (7). Systems for CSP hardware development have been built to replicate both the intensity and spectrum of focused sunlight (Figure 6).

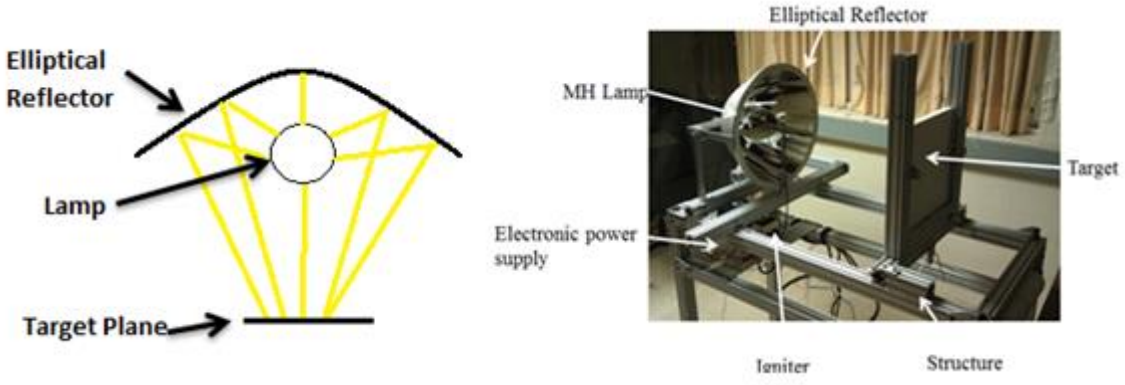

Figure 6: 2D rendering and physical model of a solar simulator used to concentrate light (8)

The function of a concentrating solar energy system is to focus sunlight over a small area and convert the solar energy to heat. This may be achieved with elliptical reflectors because of their optical properties: light emitted from a lamp at one focal point will be redirected off the reflector and pass through the second focal point, where the target plane is strategically placed. The power requirements for the simulator in are 1.5 kW and can produce intensities up to 600 kW/m^2 (600 suns) CSP serves many applications, but the focus of this study requires collimated light from the system (17).

The last category of solar simulators are systems that emit collimated light over the solar spectrum with a uniform intensity (Figure 7).

Figure 7: 2D rendering and physical version of a solar simulator using parabolic mirrors to collimate light (10)

Systems that collimate light typically use a lamp and parabolic reflector. The diffuse light is emitted from the lamp at the focal point and captured by the reflector where it is subsequently collimated. These systems rely on the optical properties of parabolic mirrors to collimate the light (Figure 8).

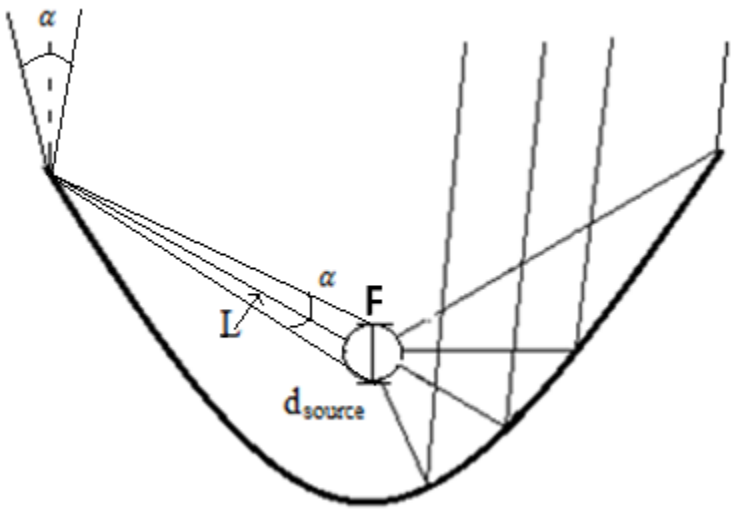

Figure 8: A parabolic mirror where a light source larger than zero is emitting light from the focal point (F) resulting in an angular divergence, α

The light emitted from the focal point, F, becomes collimated when it reflects off of the parabolic mirror. In theory, F is an infinitesimally small point, while in practice the light can be released from very close to this point, but not at the exact location. The more compact a light is, the smaller the resulting divergence is.

Optical Energy Technologies has developed a platform capable of emitting light at a 17.5 mRadian divergence, or approximately double that of natural sunlight (Figure 8). The system produces an intensity on the target plane of 1150 kW/m^2 with a diameter of 660 mm and emits light similar to the solar spectrum (10). The specifications make it a suitable option for testing optics, however the cost of $36,000 make it unattainable for Bucknell University, as well as other small teaching and research institutions.

The three classes of solar simulators serve many applications. The criteria for this project require the light to be collimated, and as a result, only the last category of simulators could be used. The literature review indicated that a metal halide arc lamp would provide a good approximation of

the solar spectrum. Additionally, high quality electroformed reflectors are commercially available for prototype systems, specifically from the company Optiforms (9).

Methods

Concept Development and Analysis

Previous research for low divergence solar simulators has been primarily limited to hardware comprised of a light source and parabolic reflector. Two simulator concepts were considered: a parabolic reflector with an arc-lamp source, and reflector with an arc-lamp source and a light collimator. The parabolic reflector was considered because of its optical properties (i.e. produces nearly parallel rays from a diffuse source) and successful implementation in previous solar simulators, most notably in spotlights. This concept showed promise of being cost efficient while delivering an accurate solar spectrum, uniform intensity and low angular divergence. What the model must consider is how the geometry affects performance, which can be analyzed most effectively with a simple model. Before deciding on building the lamp and reflector model, another concept with a geometric collimator was evaluated to assess any possible performance gains.

The collimated parabolic mirror concept is shown in Figure 9. The addition of the collimator results in a system where the light hitting the target plane remains under a predefined angular divergence.

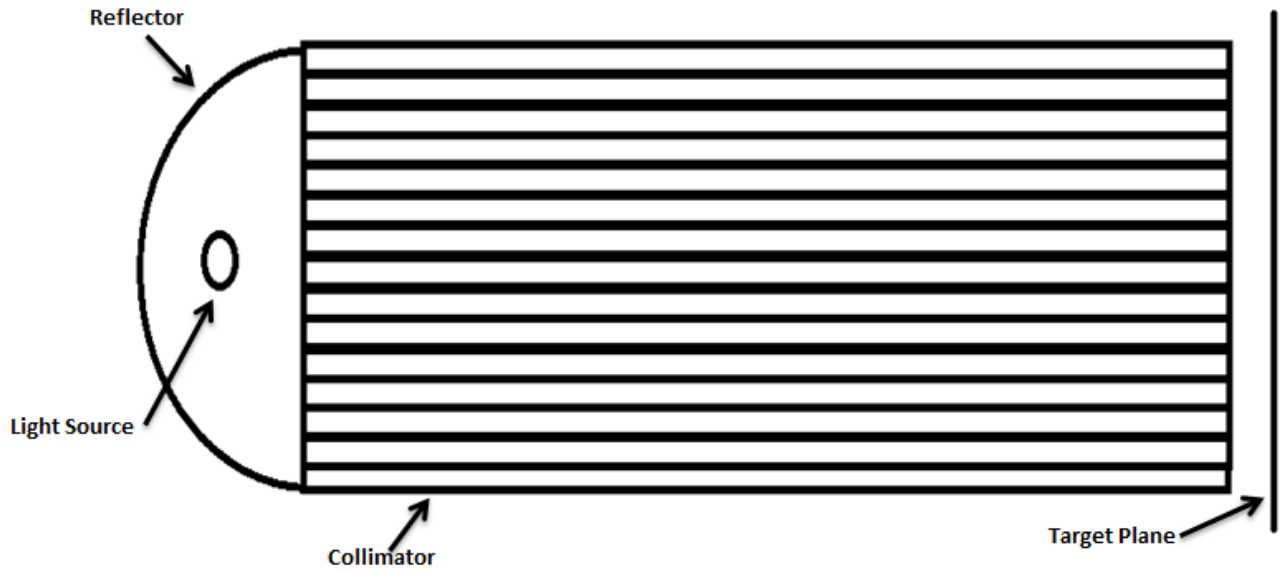

Figure 9: Two dimensional rendering of a collimator that consisting of long, slender tubes that filter light over a predetermined angular divergence

The collimator is essentially a light filter. Rigid tubes are arranged in parallel to construct the collimator and would absorb light that was incident to their sides. Light that does not come into contact with the tube wall would exit the other end onto the target plane as a collimated beam. The maximum angular divergence can be controlled, as it is a function of both the collimator's length and tube diameter (Appendix I). Subsequently, the model would also be compatible with diffuse light sources.

The collimator and lamp and reflector concepts had different advantages, but the primary concerns for the system were the angular divergence and the transfer efficiency. Transfer efficiency is defined as the amount of light (energy or power) hitting the target plane divided by the total amount of light emitted. The target angular divergence could be reached with the addition of the collimator. In order to achieve an angular divergence of 9.2 mRadians, the required length of the collimator would be 0.8 meters (using 7 mm diameter tubes). Most of the light entering the collimator would be subsequently absorbed by the walls, resulting in a transfer

efficiency of 1.8%. The power requirements to provide at least 600 W/m^2 would need a 33.4 kW light source which would be too robust and expensive for practical purposes. As such, this concept was discarded and subsequent design efforts focused on the parabolic reflector configuration without a collimator.

Development of the geometric model

All of the parameters studied are related to geometry because it is assumed the shape and location of the parts in the system would have the largest impact on performance. A model was developed in MATLAB to evaluate different configurations of a lamp and parabolic reflector system shown in Figure 10. The parameters varied in the model include the source size (d_{source}), the aperture size, (D_{app}), and the rim angle, (ϕ_{rim}).

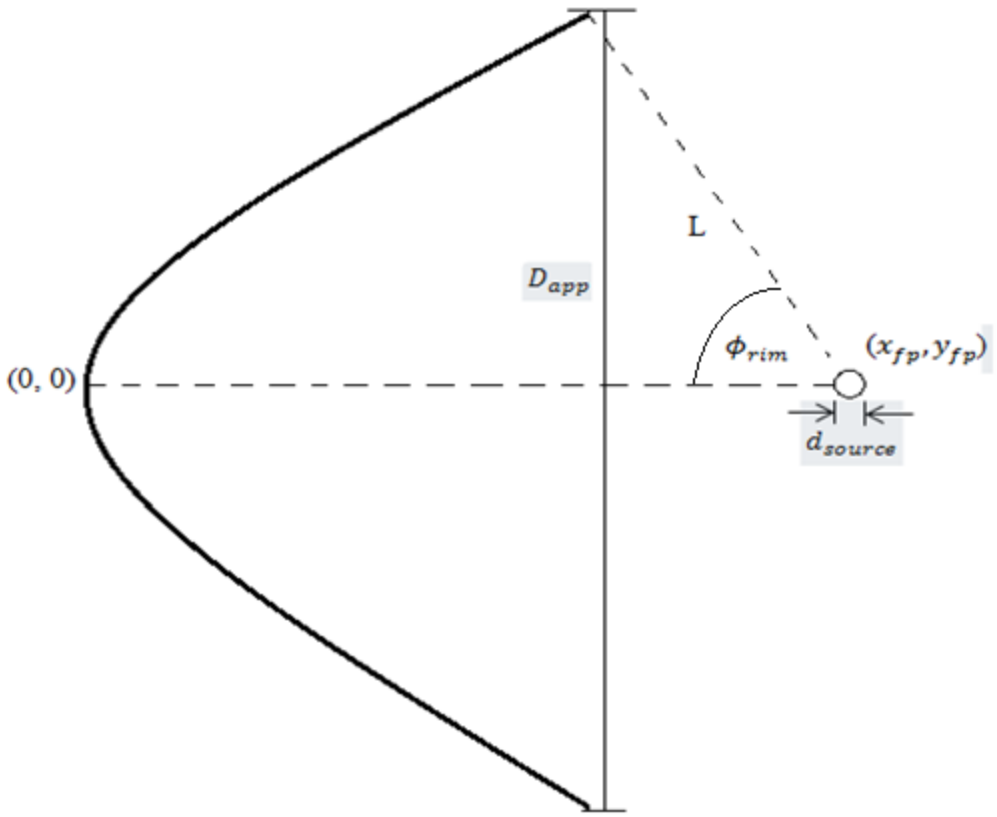

Figure 10: The parameters used to develop a mathematical model for the angular divergence and efficiency of the lamp and reflector combination

The vertex of the reflector was assigned the coordinates (0,0). D_{app} is defined as the parabolic reflectors aperture diameter. The placement of the lamp is located at the x and y coordinates of the focal point, (x_{fp}, y_{fp}) and the diameter of the lamp is denoted d_{source}. The focal point of the paraboloid dictates the aperture position and rim angle, ϕ_{rim}, which is also the angle between the edge of the paraboloid and the vertex. The distance from the focal point to the edge of the reflector is defined as L. These parameters are used to determine the angular divergence of lamp and reflector model (Appendix II). The maximum divergence was found to be the result of two light beams from both ends of the arc hitting the outer edge of the reflector, resulting in a divergence of α (Figure 11).

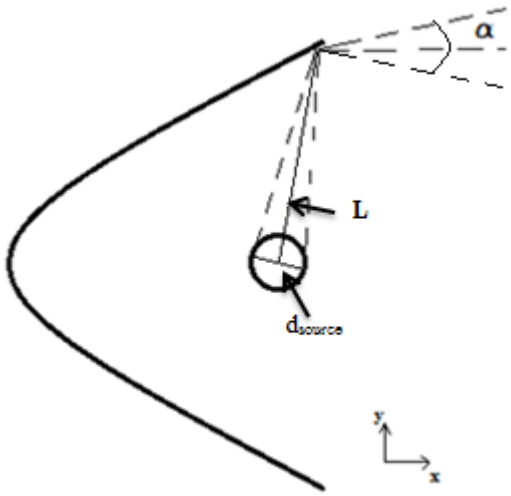

Figure 11: The maximum angular divergence of light from a parabolic reflector

By measuring the distance from the source to the edge of the reflector, L, and knowing the source diameter, d_{source}, the maximum angular divergence, α, could be calculated with the expression

$$\alpha = 2\frac{atan(\frac{d_{source}}{2})}{L} \quad (1)$$

Equation 1 shows the angular divergence can be improved by increasing L (e.g. increasing the size of the aperture) or decreasing d_{source}. Since it is also necessary to have a system with a high efficiency, methods are developed to see parameter effects on the transfer efficiency. View factors are used to estimate the transfer efficiency because they are commonly used in heat transfer for evaluating the transport of radiant energy (e.g. light) (Figure 12). Their function is to measure the exchange of energy between two surfaces and can be capable of modeling complicated scenarios with relatively simple formulas.

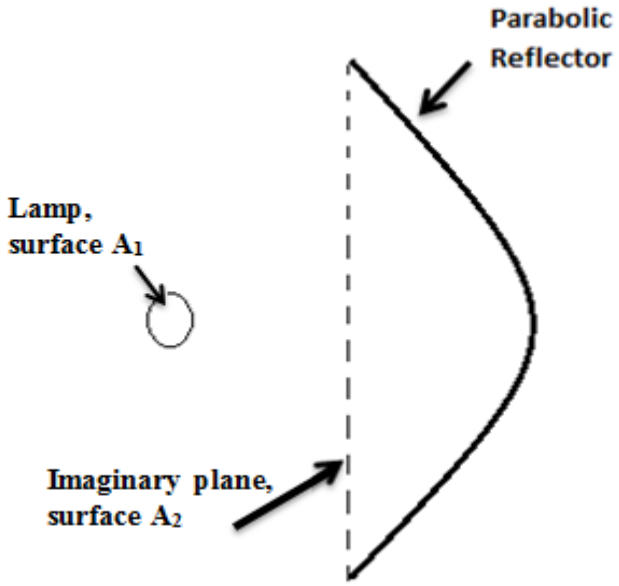

Figure 12: The efficiency for a lamp and reflector system depends on how much light from the lamp "hits" the imaginary surface on the opening to the reflector

The lamp, surface A_1, is emitting light as a point source. View factors can be used to estimate how much of that light is incident on surface A_2, all of which is assumed to strike the reflector surface. The amount of diffuse light reaching surface A_2 compared to the total amount of light is the transfer efficiency. Subsequently, the lamp and reflector's efficiency is defined as of the amount of light emitted from the lamp that hits the surface of the reflector,

and can be found with the equation

$$F_{12} = \frac{1}{2}\left(1 - \frac{1}{\sqrt{1 + \frac{1}{h^2}}}\right) \quad (2)$$

F_{12} is the transfer efficiency and *h* is the distance from the light source to the imaginary surface divided by the reflector's diameter (12). If the lamp is located on the other side of the imaginary

surface (in the dish), view factors could still be used. The efficiency would then be defined as the proportion of light that does not hit the imaginary surface to the total amount of light. When the lamp is inside the dish, the efficiency would exceed 50% because over half the light emitted would be incident on the reflector.

Results

MATLAB

A parametric analysis was conducted in MATLAB to evaluate the lamp and reflector concept using the previously discussed optical model. The mathematical models showed that the angular divergence was a function of source size and the distance from the lamp to the edge of the reflector. Therefore, a range of reflector diameters (0.05, 0.1, 0.2, 0.5, 1 and 2 meters) were all evaluated at rim angles of 15°, 30°, 45°, 60°, 90°, and 120° to observe the trends between rim angle and reflector diameter (Figure 13).

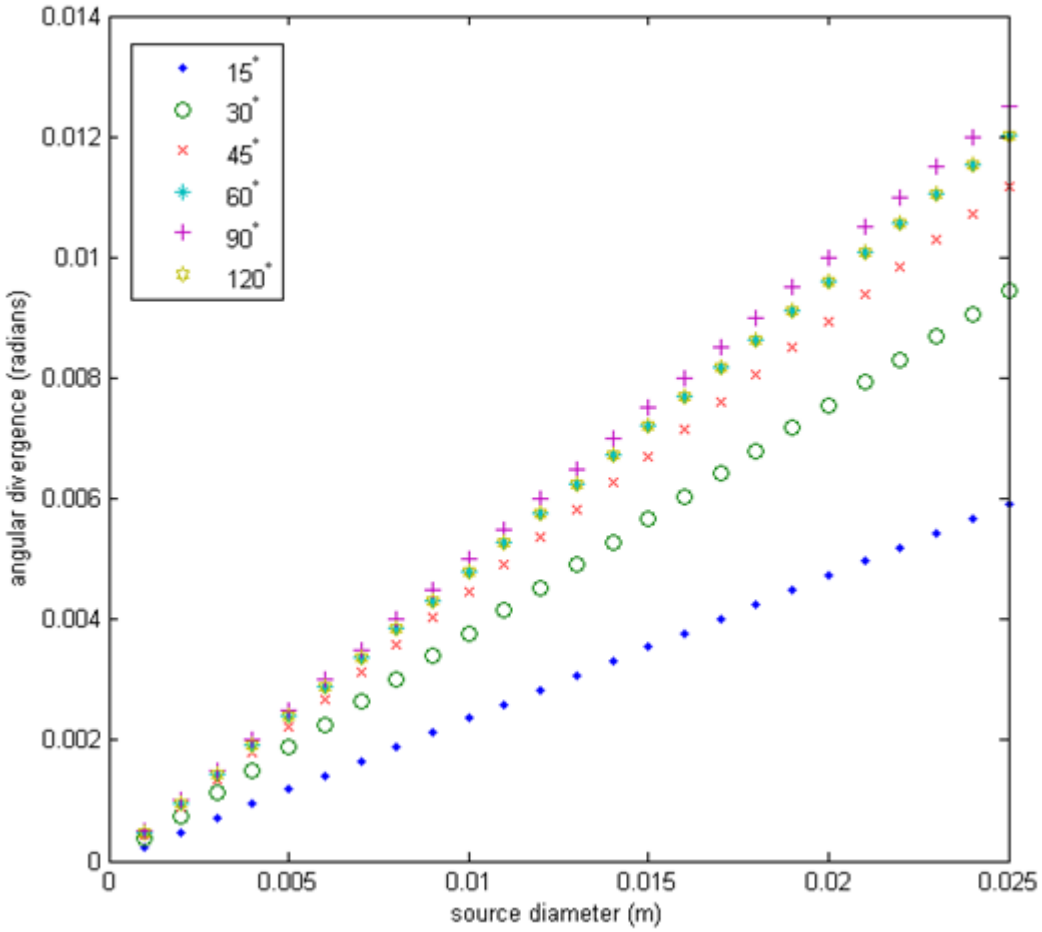

Figure 13: The angular divergence as function of source diameter for a reflector with a 2 meter diameter

When the source size increases, the angular divergence does as well. Additionally, as the rim angle increases, the angular divergence does as well. Each rim angle has a different slope, the angular divergence for a rim angle of 15° increases at the smallest rate, and an increase in rim angle increases the rate at which the angular divergence rises; rim angle puts the lamp further away from the reflector, and subsequently redirects the light at a lower divergence. The angular

divergence was then tabulated for every reflector diameter and rim angle with source sizes of 5 and 9.5 mm^2 (Table 2, 3).

Table 2: The angular divergence using a mathematical model of a 5 mm source in a lamp and parabolic reflector configuration for varying angles of aperture and reflector diameter, where "suitable" divergences (under 25 mRadian) are highlighted in green

Aperture diameter (m)	15°	30°	45°	60°	90°	120°
0.05	0.052	0.100	0.141	0.173	0.199	0.173
0.1	0.026	0.050	0.071	0.087	0.100	0.087
0.2	0.013	0.025	0.035	0.043	0.050	0.043
0.5	0.005	0.010	0.014	0.017	0.020	0.017
1	0.003	0.005	0.007	0.009	0.010	0.009
2	0.001	0.002	0.004	0.004	0.005	0.004

Table 3: The angular divergence using the mathematical model of a 9.5 mm souce in a lamp and parabolic reflector configuration for varying angles of aperture and reflector diameter, where "suitable" divergences (under 25 mRadian) are highlighted in green

Aperture diameter (m)	15°	30°	45°	60°	90°	120°
0.05	0.098	0.189	0.267	0.326	0.376	0.326
0.1	0.049	0.095	0.134	0.164	0.189	0.164
0.2	0.025	0.047	0.067	0.082	0.095	0.082
0.5	0.010	0.019	0.027	0.033	0.038	0.033
1	0.005	0.009	0.013	0.016	0.019	0.016
2	0.002	0.005	0.007	0.008	0.009	0.008

[2] Metal halide lamps are available with arc sizes between 5 and 25 mm

The angular divergence in Table 2 decreased as the aperture diameter increased. While the same trend was observed for the two source sizes, the angular divergence was approximately twice as large for the 9.5 mm lamp. In order to achieve the required angular divergence for the 9.5 mm lamp, a reflector with a larger aperture diameter was necessary in comparison to the 5 mm source. For both cases, reflectors with aperture diameters less than 0.2 meters did not have an angular divergence under 25 mRadians. The angular divergence was then modeled as a function of aperture diameter to observe the trend and determine the minimum aperture diameter needed to produce the desired angular divergence (Figure 14).

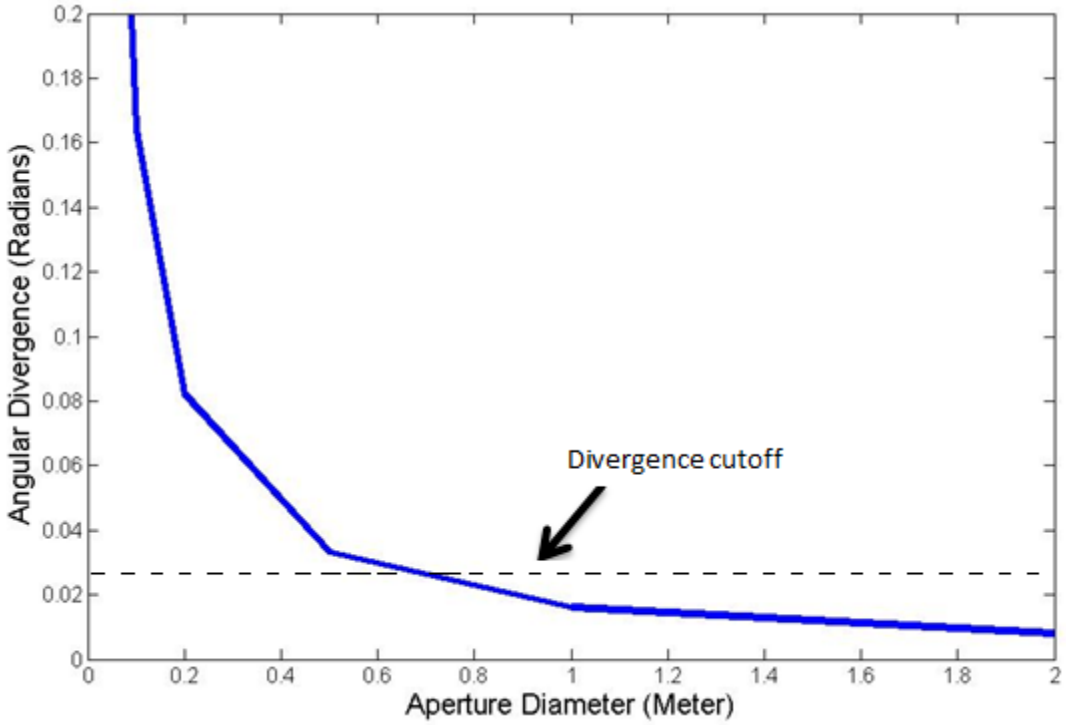

Figure 14: Angular divergence as a function of aperture diameter for a model with a rim angle of 120° and a source diameter of 9.5 mm

The angular divergence decreased rapidly until the aperture diameter approached 0.5 meters. After the diameter reached 0.5 meters the divergence began to stabilize and asymptotically approach zero. The preliminary calculations were used to understand which combinations

provided acceptable angular divergences, but the transfer efficiency was also considered in the selection process. View factor calculations showed that the aperture diameter was irrelevant and the rim angle alone influenced the transfer efficiency (Table 4).

Table 4: The transfer efficiency for varying angles of aperture and diameter, independent of source size

Aperture diameter (m)	**15°**	**30°**	**45°**	**60°**	**90°**	**120°**
0.05	0.02	0.07	0.15	0.25	0.50	0.64
0.1	0.02	0.07	0.15	0.25	0.50	0.64
0.2	0.02	0.07	0.15	0.25	0.50	0.64
0.5	0.02	0.07	0.15	0.25	0.50	0.64
1	0.02	0.07	0.15	0.25	0.50	0.64
2	0.02	0.07	0.15	0.25	0.50	0.64

Table 4 shows that the transfer efficiency increased as the rim angle increased. This can be attributed to the reflector capturing more of the emitted light, which in turn requires less power to transmit the same amount of energy onto the target plane (Figure 15).

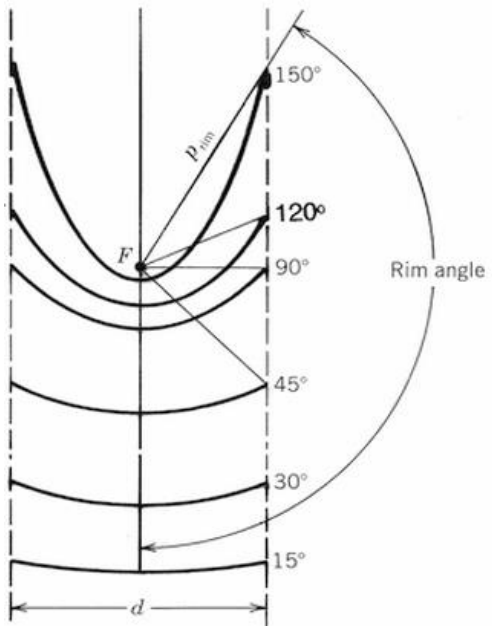

Figure 15: The rim angle's influence on the distance from the focal point to the reflector

Figure 15 shows how larger rim angles affect the shape of the reflector and dictate the distance from the focal point the reflector. For smaller rim angles, the reflector is flatter while the focal point is located outside of the dish. For large rim angles, specifically over 90°**,** the reflector is curved, and the focal point is located inside the reflector.

The results and trends from the geometrical model were compared TracePro simulations for validation.

Model Validation Using TracePro

TracePro was used to validate the geometrical model due to ray tracing's ability to simulate thermal and optical systems. The solar simulator was modeled with the same aperture diameters and rim angles as the MATLAB to be for comparison (Figure 16).

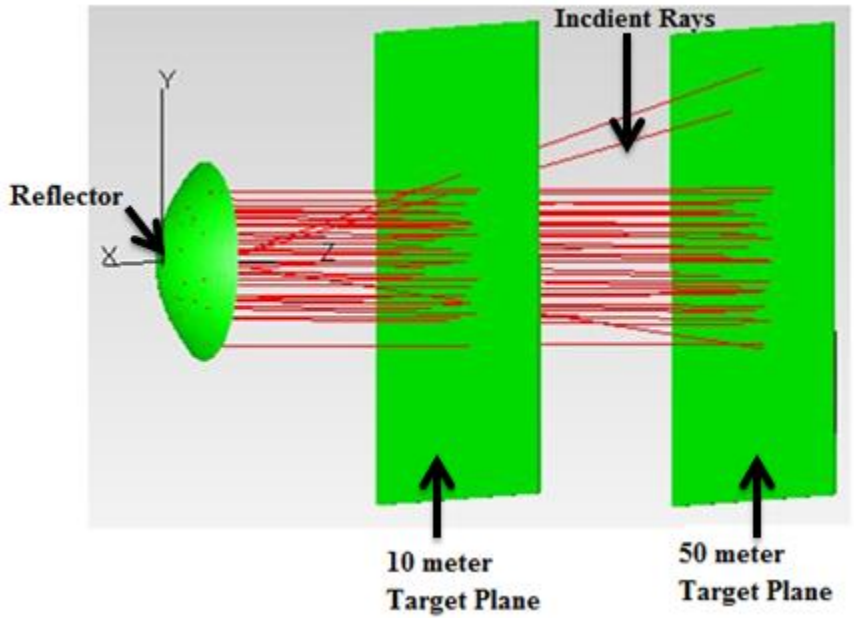

Figure 16: Ray tracing for a system with a 0.5 meter aperture with a rim angle of 90° with the rays projected onto 10 and 50 meter target planes (not modeled to scale)

Ray tracing using TracePro was advantageous because of the data it provided along with visual models. Ray tracing is simulated with an algorithm that randomly generates vectors off of a surface (20). Optical properties can also be assigned to simulated objects, which influence the ray's behavior. One standard application for ray tracing, and specifically TracePro is to model optical equipment, such as telescopes and cameras (19) (Figure 17).

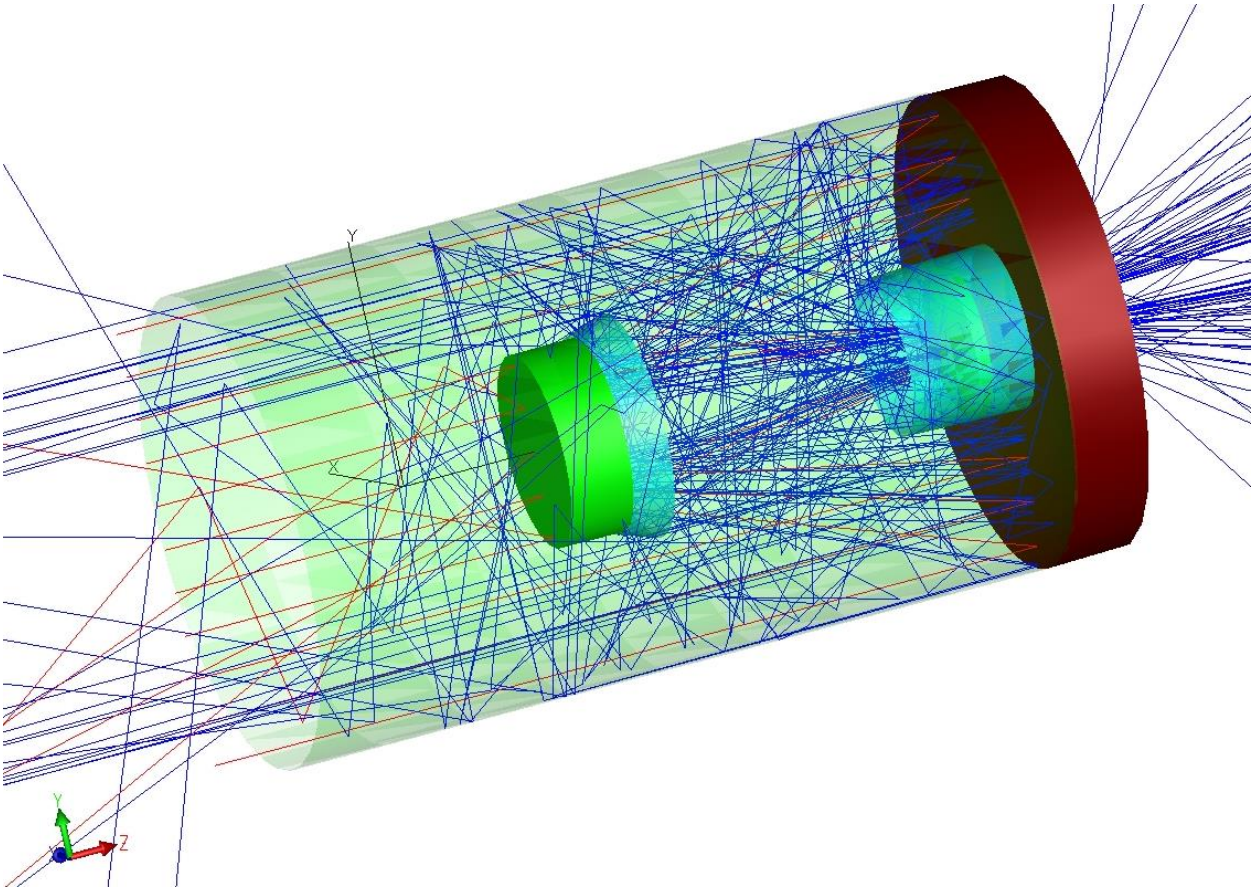

Figure 17: An analysis of a telescope in TracePro (19)

Figure 17 shows a simulation of the James Webb Space Telescope currently being built by NASA. Telescopes accommodate light over a range of wavelengths through the use of mirrors and lenses, not unlike the parabolic reflector used for a solar simulator. After looking at the complicated analyses performed in TracePro, it was assumed that it would be an acceptable tool to validate the geometrical model of a parabolic reflector. Whereas MATLAB is used to solve equations, TracePro can evaluate CAD models and simulate its use through algorithms to generate data.

The angular divergence of each reflector and lamp combination was calculated by placing target planes at 10 and 50 meters from the reflector and directing the light towards them. The divergence was calculated by determining the increase in the diameter of the light beam between the 10 and 50 meter plane and measuring the slope between the two projections (Figure 18).

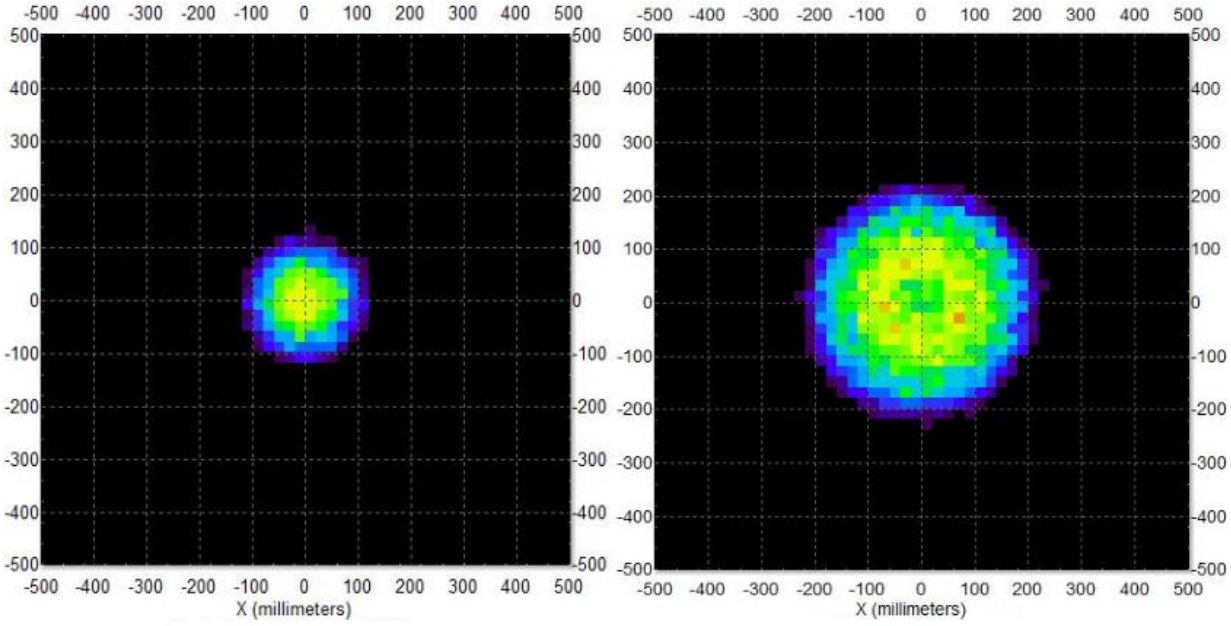

(a) (b)

Figure 18: Intensity mappings in TracePro for target planes at a) 10 meters, and b) 50 meters.

The angular divergence can be calculated with the two diameters

In order to find the angular divergence, the diameter of the projected light was found from the intensity map. The increase in diameter and the distance between the two planes provided enough trigonometric information to calculate the angular divergence (Table 5, 6). While the diameter measurements of the projected light were not exact, they provided an approximation for the angular divergence of each configuration.

Table 5: The angular divergence using a 5 mm source in a lamp and parabolic reflector configuration for varying angles of aperture and reflector diameter, where "suitable" divergences (under 25 mRadian) are highlighted in green

Aperture diameter (m)	**15°**	**30°**	**45°**	**60°**	**90°**	**120°**
0.05	0.050	0.105	0.150	0.194	0.160	0.140
0.10	0.025	0.050	0.075	0.099	0.154	0.080
0.20	0.010	0.025	0.035	0.055	0.080	0.115
0.50	0.005	0.005	0.010	0.020	0.030	0.045
1.00	0.000	0.005	0.010	0.005	0.010	0.015
2.00	0.000	0.000	0.000	0.000	0.000	0.000

Table 6: The angular divergence for a 9.5 mm source in a lamp and parabolic reflector configuration calculated in TracePro for varying angles of aperture and reflector diameter, where "suitable" divergences (under 25 mRadian) are highlighted in green

Aperture diameter (m)	**15°**	**30°**	**45°**	**60°**	**90°**	**120°**
0.05	0.080	0.194	0.278	0.432	0.278	0.630
0.10	0.040	0.080	0.160	0.199	0.160	0.395
0.20	0.040	0.040	0.080	0.120	0.160	0.278
0.50	0.002	0.010	0.030	0.040	0.070	0.200
1.00	0.000	0.005	0.005	0.015	0.025	0.045
2.00	0.000	0.005	0.005	0.005	0.005	0.005

The results from TracePro show good agreement with the values calculated using the MATLAB model (Figure 19).

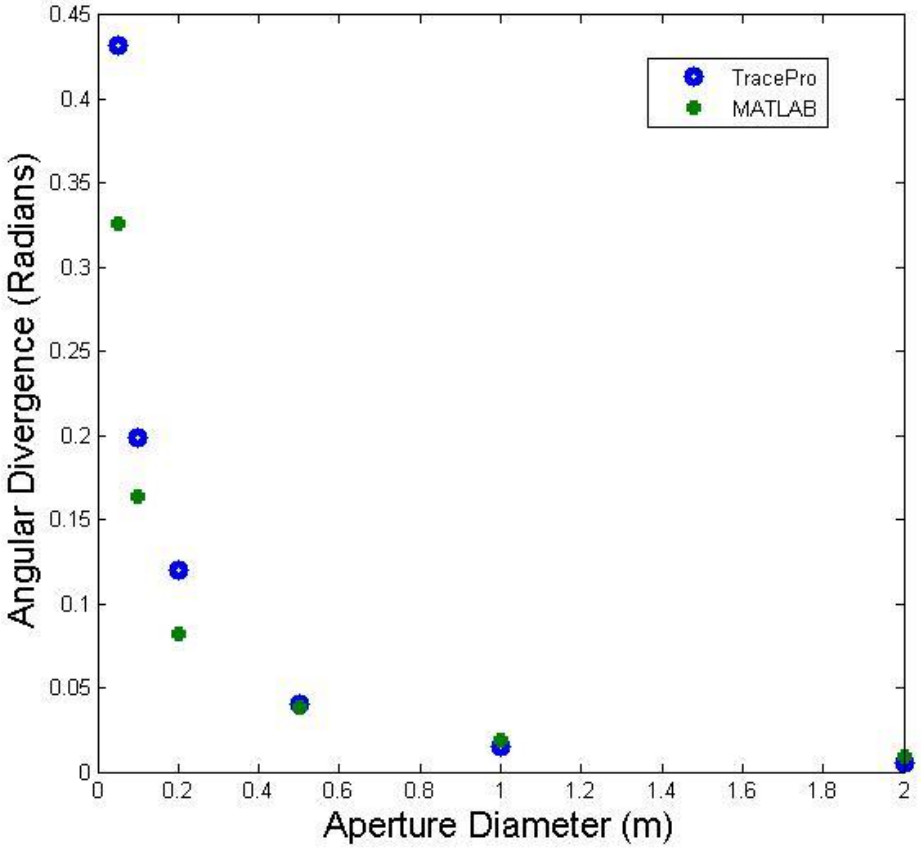

Figure 19: Angular divergence as a function of aperture diameter comparison between the MATLAB and TracePro results for rim angle of 90°

Despite slightly different numerical values, the comparison between the MATLAB and TracePro results share the same trend. For smaller aperture diameters the difference is large, specifically 0.106 radians for an aperture diameter of 0.05 meters. As the aperture diameter increases, the discrepancy between the two values decreases to 0.004 radians for diameters of 1 and 2 meters. Slight differences were expected, as the MATLAB model was an approximation used solely for a preliminary assessment. Minor inconsistencies between the angular divergences for larger aperture diameters were considered acceptable. As such, the transfer efficiencies were subsequently evaluated in TracePro and compared to the MATLAB models (Table 7).

Table 7: The efficiency of the lamp and reflector configuration modeled in TracePro for a 9.5 mm source projected onto a target plane 10 meters away

Aperture diameter (m)	**15°**	**30°**	**45°**	**60°**	**90°**	**120°**
0.05	0.08	0.12	0.19	0.29	0.55	0.79
0.1	0.08	0.12	0.19	0.30	0.55	0.80
0.2	0.09	0.13	0.20	0.30	0.56	0.80
0.5	0.09	0.13	0.21	0.31	0.56	0.80
1	0.11	0.14	0.22	0.32	0.56	0.80
2	0.15	0.15	0.22	0.32	0.56	0.81

The values in Table 7 were provided by TracePro and no calculations were necessary. While the efficiency increased as the rim angle increased, there was a slight variation in the results. In the MATLAB simulation, the efficiency was not a function of aperture diameter. In the TracePro models, the efficiency increased as the aperture diameter increased, with the effect diminishing as the rim angle was increased. The discrepancy can be attributed to the fact that the MATLAB calculations used view factors, which are approximations to determine the amount of radiative heat transfer occurring and may have limitations based on the relative size of the surfaces considered. The efficiencies were then compared for the MATLAB and TracePro results for a 0.5 meter aperture diameter because commercially available reflectors are typically about this size (Figure 20)

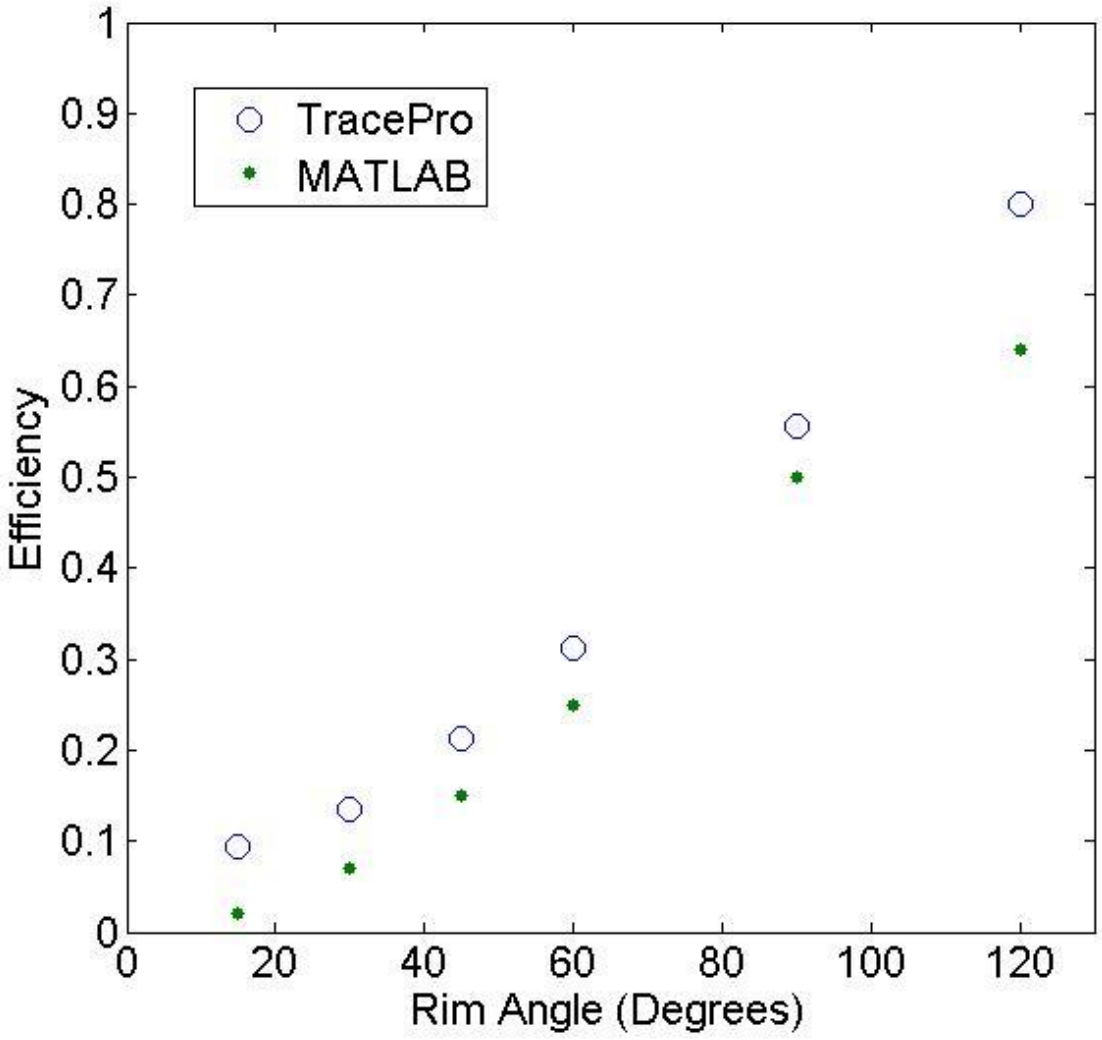

Figure 20: The efficiency as a function of rim angle in MATLAB and TracePro for a reflector with a 0.5 aperture diameter

Figure 20 shows a similar trend, although the MATLAB results are steadily provide an efficiency that is approximately 5% lower than the TracePro results. Although the view factor approach used in MATLAB underestimate the efficiency, it consistently underestimates it. Figure 20 shows that for rim angles 90º or larger, the efficiency exceeded the project objective of an efficiency greater than 40%. As such, based off of the geometrical approach, one can

confidently build a solar simulator under the assumption the system will have an efficiency that is about 5% higher. Subsequently, if the power output by the actual system is too high because of the lower efficiency estimations, less voltage can be supplied to the system to lower the output, and generate results consistent with the geometrical model.

The results from the geometrical model indicated that a platform meeting the angular divergence and efficiency requirements could be built. The TracePro models confirmed this, and the trends for both models were evaluated to determine what equipment to buy for the prototype.

Design Recommendations

The preceding model results mapped out the design space. The angular divergence was heavily influenced by the aperture diameter and source size, with the best performance achieved by maximizing the ratio of aperture size to source diameter. The efficiency of the system started to level off at a rim angle of 90°, before increasing again. While making the rim angle larger than 90° would increase efficiency, it would come at the cost of practicality. Therefore, a prototype was recommended to have a rim angle of approximately 90° radians with an aperture diameter of at least 0.5 meters. A metal halide lamp was chosen because it is cost effective and its representation of the AM 1.5 spectrum was deemed acceptable. A smaller source diameter would have lowered the angular divergence, but compromises had to be made in order to meet the power requirements. About 1000 W was needed to be projected onto the target plane to reach the required intensity and with a 40% efficiency, a 2.5 kW lamp be required. 2.5 kW Metal halide lamps are available and have a 9.5 mm diameter.

Prototype Design

While the geometric model and TracePro results influenced the design of the system, previous works also provided information for selecting parts. The solar concentrator at Bucknell University provided some information for vendors for lamps and reflectors. The system uses a 1,500 W Metal Halide lamp from Osram. Higher power lamps were considered for the concentrator, as it was noted a common source diameter for a 2,500 W lamp was 14 mm, and the smallest being 9.5 mm. As a result, the lamp chosen for the solar simulator in this study prototype was a 2.5 kW, 9.5 mm metal halide arc lamp. The reflector in the solar concentrator was elliptical, and cost $1,300 (16). While a parabolic reflector was needed for this study, the same vendor, Optiforms, also manufactures these. Optiforms was contacted, and their largest parabolic reflector, the p174-100, had a 635 mm diameter mirror with a reflectivity of 0.97 and a focal length of 174.5 mm for $1,600. Optiforms customized the design by adding a 100 mm hole centered on its vertex where the 2.5 kW, 9.5 mm diameter metal halide lamp could be supported for testing (Figure 21).

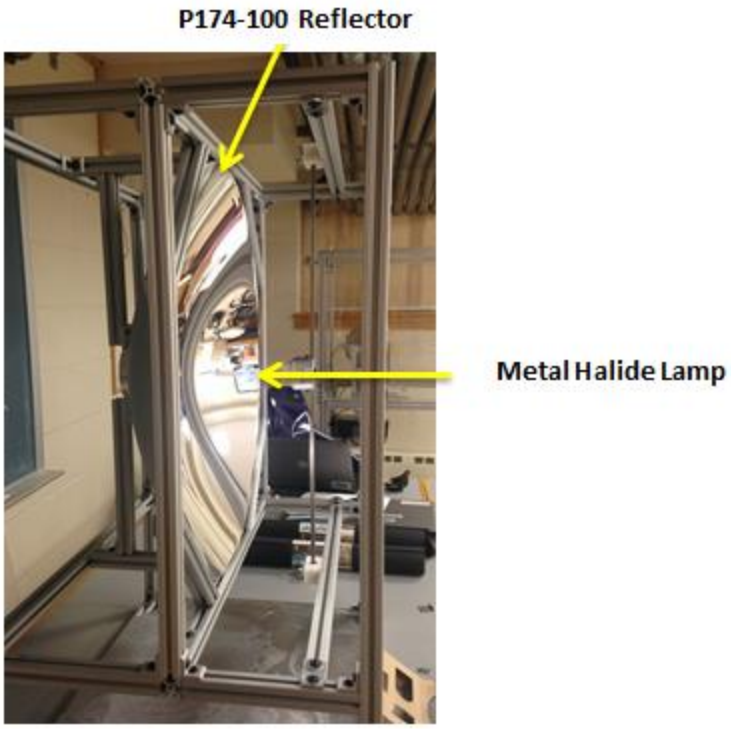

Figure 21: p174-100 reflector and metal halide lamp assembled in its housing

The model was arranged such that the reflector was housed within a frame. The lamp was secured with a cross beam in front of the reflector at the location of the focal point. In order to power the prototype, a ballast was required. Although the initial target was to develop a prototype for under $3,000, the cost of the entire system exceeded this (Table 8).

Table 8: Bill of materials for the prototype

Item	**Cost ($)**
Reflector	1,800
Lamp	450
Ballast	756
Structure	250
Total	3,256

Prototype Validation using TracePro

For the evaluation, a more accurate method to measure the angular divergence was developed. Target planes were placed 10 and 50 meters away from the model, and the angle of incidence of the light rays hitting the target planes was measured. The angle of incidence for the rays was averaged to find the mean angular divergence produced by the system (Table 9).

Table 9: TracePro results for the p174-100 reflector with a 2.5 kW 9.5 mm source

Target Plane	**10 Meters**	**50 Meters**
Average Angular Divergence (mRadians)	38.6	19.5
Standard Deviation (mRadians)	23.3	0.088
Transfer Efficiency (%, Watts)	46.2, 1156	40.8, 1021

The results show that angular divergence decreased as the distance to the target plane increased. Additionally, the standard deviation decreased, indicating the rays were restricted to a much smaller angular divergence range. The efficiency also declined as the distance increased due to rays with a high angular divergence not hitting the target plane. The amount of light hitting the 10 and 50 meter planes was 1156 W and 1021 W, respectively. The angle of incidence was also calculated for every ray hitting the target planes. At 10 meters the mean divergence was 38.6 mRadians with a standard deviation of 23.3 mRadians. At 50 meters the average divergence was 19.5 mRadians with a standard deviation of 0.0885 mRadians. As the target plane moved farther away, the standard deviation decreased due to rays with higher angular divergences missing the target entirely (Figure 22).

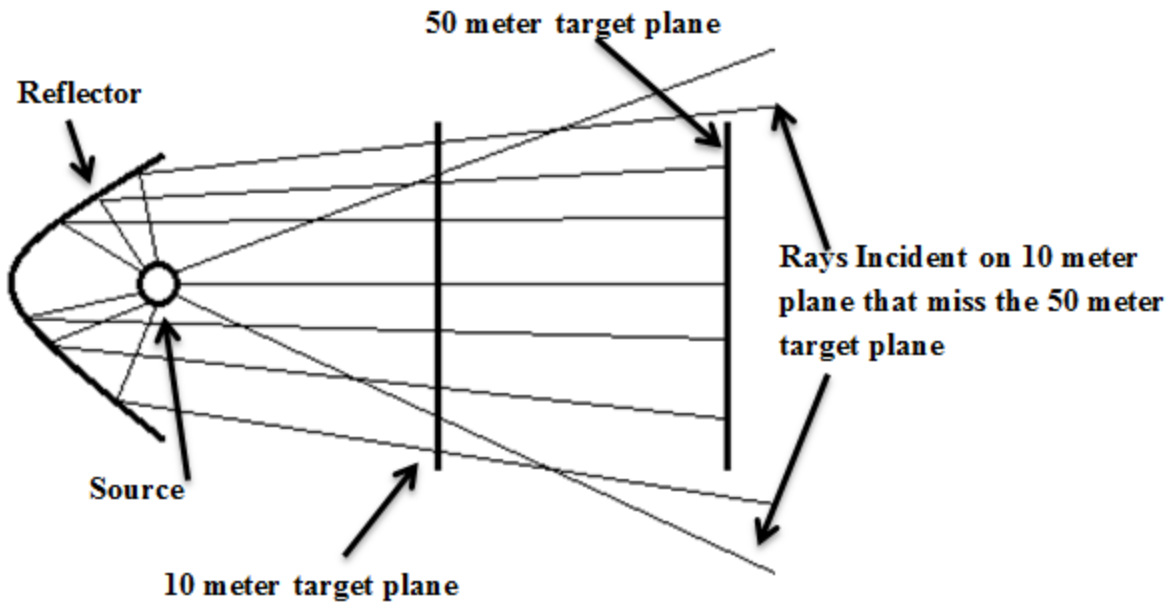

Figure 22: Light rays with larger angular divergences incident on the 10 meter plane but miss the 50 meter target plane entirely

Figure 22 shows how rays with larger angular divergences will be incident on planes close to the reflector, but will miss planes further away. As such, when these rays are not incident on the target plane, the mean and standard deviation lower and produce a more uniform angular divergence. Furthermore, to determine the uniformity of the angular divergence on both target planes, the distribution of the divergence values were evaluated. The range of $\pm$ 3 standard deviations for the 50 meter target plane was 19.23 – 19.77 mRadians, which corresponds to 99.7% of incident light on the plane (13). If 99.7% of the energy (1017 W) hitting the 50 meter plane was in that range, the same amount of energy would be in this range on the 10 meter plane. As such, it was deduced that at least 88% of the light on the first plane is in the span of 19.23-19.77 mRadians. To evaluate other system requirements, a flux map was created in TracePro for the size of the target plane and the intensity distribution (Figure 23).

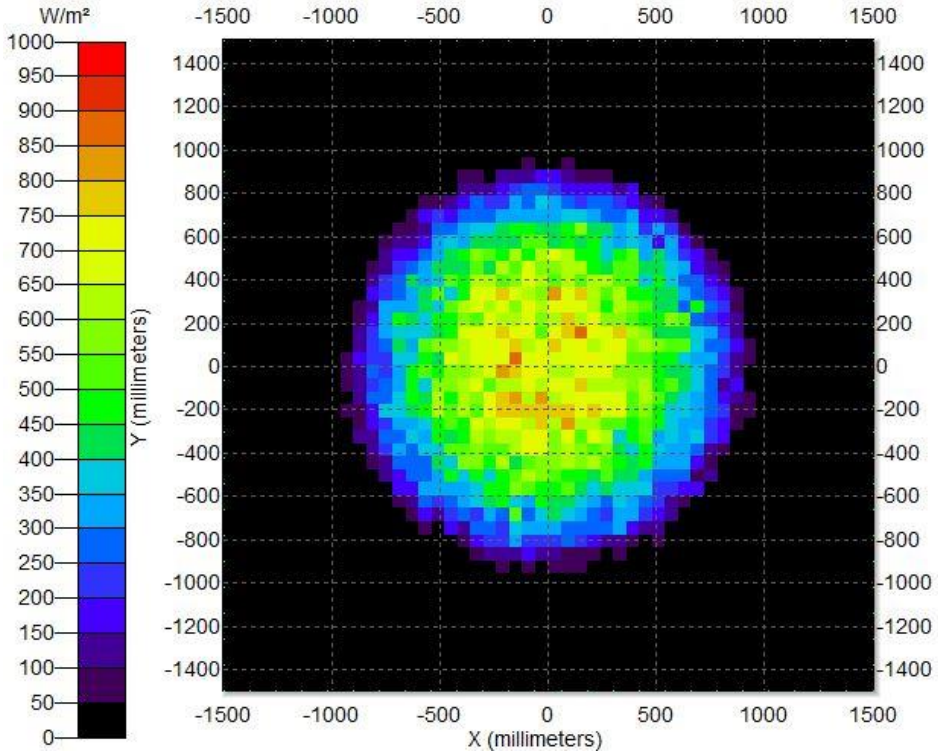

Figure 23: The flux map from the p174-100 reflector and the metal halide lamp on a target plane 50 meters away

The light on the target plane has a diameter of approximately 2 meters, more than doubling the target requirement of 0.90 meters. As for the intensity, the system requirements were 600-1000 W/m^2 over the target area. On the other edges of the projection, the intensity is less than this, but for a majority of the area, the intensity is in this range. While there is some variance in the light intensity, the model shows a fairly uniform distribution. As such, the size and intensity distribution requirement could be achieved with this system.

Additional Analysis

While previous work indicates the use of metal halide lamps as a sufficient approximation of the solar spectrum, the lamp used in the system was evaluated to ensure its accuracy. The solar spectrum is unique to an object with a color temperature of 5800 K, or approximately that of the sun. The solar spectrum can be modeled with the equation

$$E = \frac{2hc^2}{\lambda^5}\frac{1}{e^{\frac{hc}{\lambda kT}} - 1} \tag{4}$$

where h is the plank constant, k is the Boltzmann constant, c is the speed of light, and λ is the wavelength of the light. The 2.5 kW lamp from Osram had a color temperature of 6000 K, and was also modeled with Equation 4 for wavelengths ranging from 0 to 3500 nm (Figure 24).

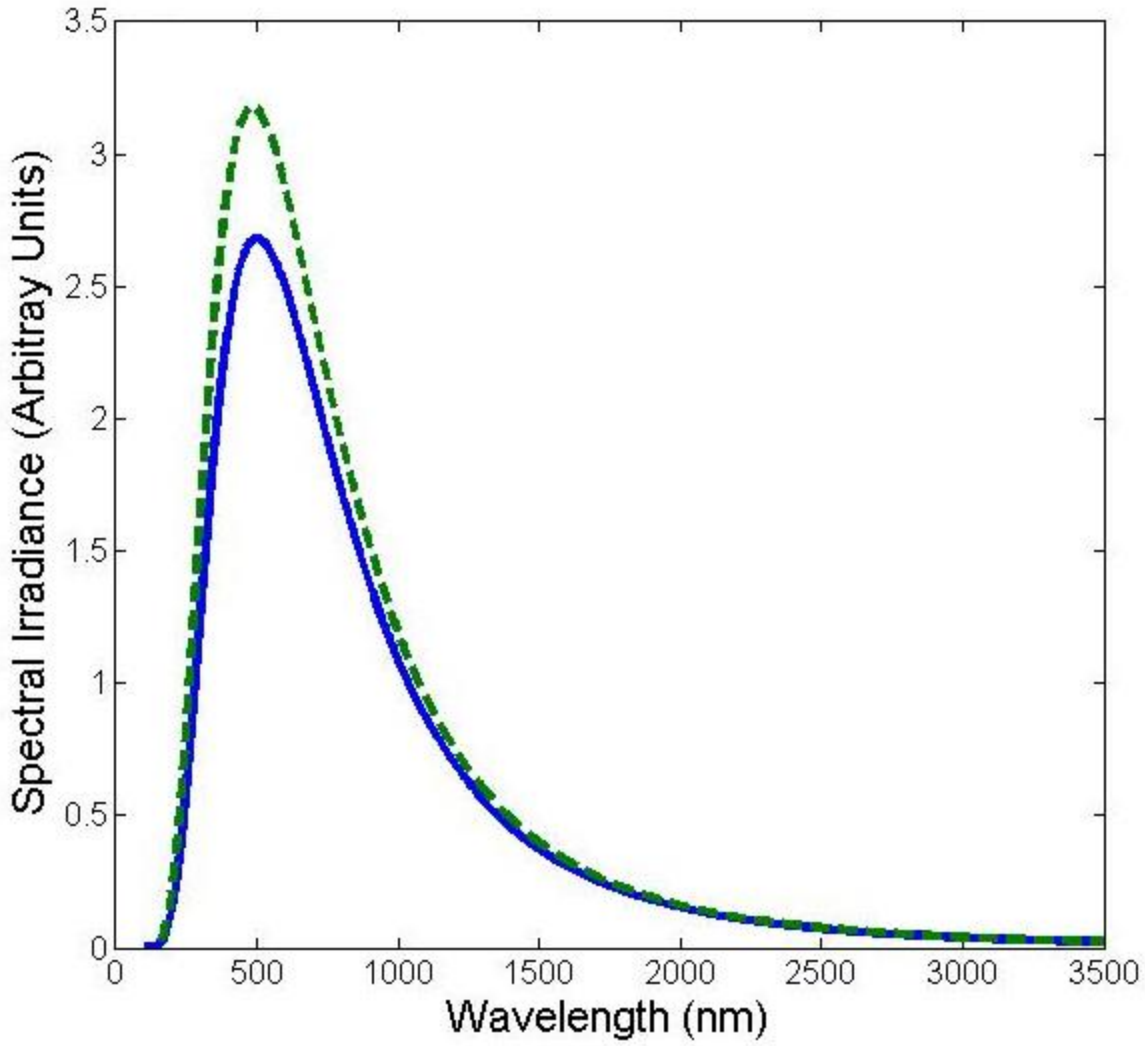

Figure 24: The spectrum produce by two objects with color temperatures of 5800 K and 6000K

Figure 24 shows the two surfaces with color temperatures of 5800 K and 6000 K following the same trend, with the largest discrepancies around wavelengths of 600 nm. To determine how well the light would model the solar spectrum, the percent error between each wavelength was calculated and then averaged (Appendix IV). The average percent error was found to be 10.9%, which was considered acceptable for the testing of optical equipment of which the properties are not sensitive to such small differences.

Another objective of this study was to develop a platform capable of producing an angular divergence equal to or less than the sun's angular divergence. The prototype's performance was predicted to fall short of the angular divergence target due to constraints related to the availability of components. This prompted an evaluation to determine the repercussions of producing an angular divergence greater than that of the sun. An application for the solar simulator would be to refocus light using optical equipment. Refocusing light can be used to measure a device's concentration factor, which is defined as the ratio between the area emitted light to the area of concentrated light. This can be tested by directing the light off of the reflector to another parabolic reflector (Figure 25)

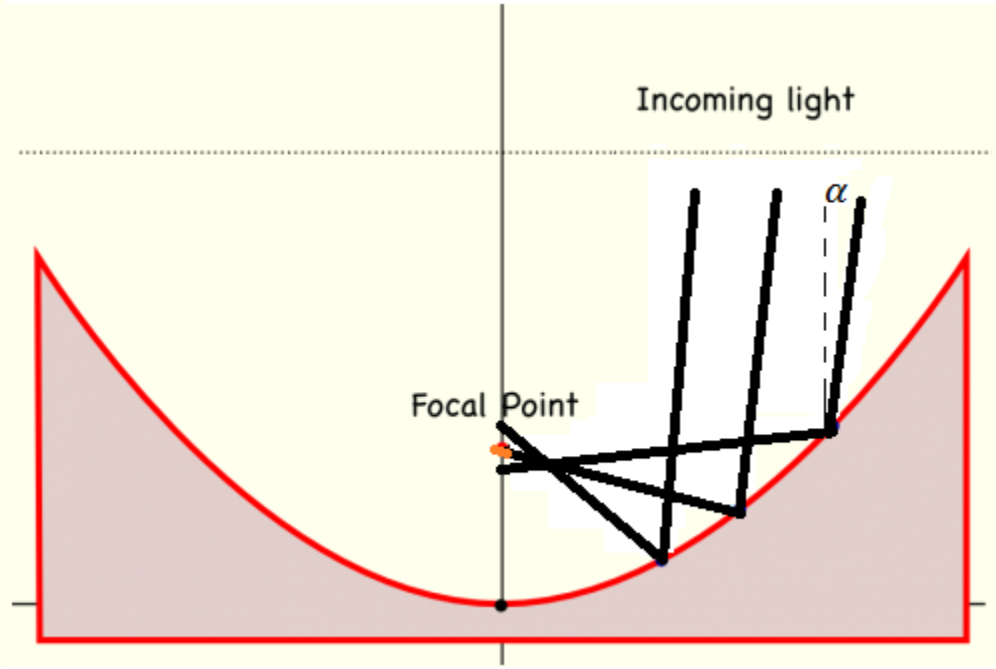

Figure 25: Incoming rays being refocused with a reflector (12)

The incoming light, if parallel would be refocused to an infinitely small point. The light produced by the solar simulator will have a divergence, and thus the refocused light will have an

area that can be used to find the concentration factor. The concentration factor can be calculated with the expression

$$C_{3D} = \frac{1}{\sin^2\left(\frac{\alpha}{2}\right)} \tag{3}$$

where ϕ_{rim} is the rim angle and α is the half angle of the incoming divergence. As the divergence increases, it spreads out and eventually impossible to refocus (Figure 26).

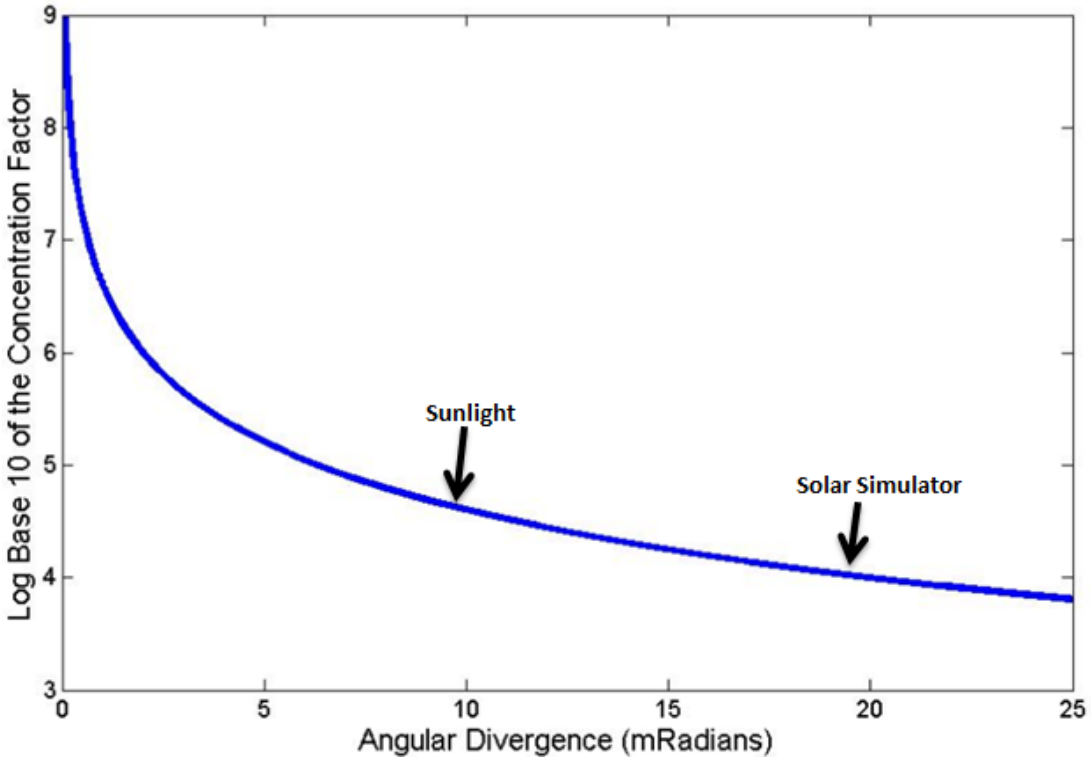

Figure 26: The logarithmic concentration factor as a function of the angular divergence for the p174-100 reflector

The concentration factor decreased rapidly as the angular divergence increased. The solar simulator produced an angular divergences in the range of 15 to 20 mRadians which

corresponded to a concentration factor of approximately 10,000, while the concentration factor for sunlight can reach 45,000 (13). For the applications of optical testing where the light will be refocused, the concentration factor would not need to exceed 1,000. As such, although the angular divergence of the solar simulator is approximately twice that of the sun, it will not hinder the testing of optical equipment.

Conclusion

Research and development is essential to the growth of solar power. Due to inconsistent sunlight in Lewisburg, PA, a solar simulator was necessary for research and educational advancement. The mathematical model evaluated in MATLAB indicated that a system could be built that would match the angular divergence of the sun. The combination of a large reflector and small light source would be capable of producing an angular divergence equal to that of the suns'. The analysis in TracePro was consistent with the preliminary assessment for rim angles larger than 45° and aperture diameters exceeding 0.5 meters.

The selection of a 9.5 mm metal halide arc lamp and p174-100 parabolic reflector was validated in TracePro (Table 10).

Table 10: Initial objectives for the project

Criterion	Angular Divergence	Average Intensity at Target Plane	Spectral Distribution Diameter	Solar Spectrum	Efficiency (%)	Cost
Target	9.2-25 mRadian	600-1000 W/m^2	0.9 Meter	AM 1.5 Spectrum	40	Less than $3,000
Achieved (Y/N)	Y	Y	Y	Y	Y	N

The efficiency depended on the location of the target plane, and had a minimum value of 40.8% on a target plane 50 meters away. Flux maps from TracePro indicated a uniform intensity over a target plane with a diameter greater than 36”. The angular divergence of the system was found to be 19.5 mRadians. While the angular divergence of the system was greater than the sun’s, the simulator was still capable of being used for optical testing, as the light could be refocused. This study provides an advancement to solar research for smaller research institutions that can develop a system from a geometrical model.

References

1. Pravettoni, M.; Norton, M.; Aitasalo, T.; Galleano, R.; Georghiou, G.; Kenny, R.P.; Barnham, K. W J, "Electrical characterization of concentrator PV cells: A comparison between outdoor testing under direct solar radiation and indoor measurements on a high intensity solar simulator," *Photovoltaic Specialists Conference (PVSC), 2010 35th IEEE* , vol., no., pp.002729,002734, 20-25 June 2010
2. Berman, T.L., Lavine, S.A., Dewitt, D.P., and Incropera, F.P., 2011, *Introduction to Heat Transfer*, 6th ed., John Wiley & Sons, Inc, Hoboken, NJ
3. Barron, A., Connexions, 2011, from http://cnx.org/content/m41217/latest/
4. Sarwar, Jawad, et al. "Description and Characterization of an Adjustable Flux Solar Simulator for Solar Thermal, Thermochemical and Photovoltaic Applications." Solar Energy 100.0 (2014): 179-94.
5. Boqer, Sede. "An Ideal Outdoor Test Environment for Photovoltaic Modules." *Ben-Gurion University of the Negev*. The Ben-Gurion National Solar Energy Center, n.d. Web. 1 Apr. 2014. <http://in.bgu.ac.il/en/solar/Pages/Services.aspx>.
6. Bazzi, A.M.; Klein, Z.; Sweeney, M.; Kroeger, K.P.; Shenoy, P.S.; Krein, P.T., "Solid-State Solar Simulator," *Industry Applications, IEEE Transactions on* , vol.48, no.4, pp.1195,1202, July-Aug. 2012
7. "Concentrating Solar Power (CSP) Technology." *Concentrating Solar Power (CSP) Technology*. Solar Energy Development Programmatic EIS, n.d. Web. 01 Apr. 2014. <http://solareis.anl.gov/guide/solar/csp/>.
8. Professorship of Renewable Energy Carriers, Department of Mechanical and Process Engineering http://www.pre.ethz.ch/facilities/vortec/
9. "Parabolic Prodcuts." *Manufacturing Electroformed Reflectors, Parabolic Reflectors, Cold Sheilds and Vacuum Coating*. Optiforms, n.d. Web. 06 Apr. 2014. <http://www.optiforms.com/parabolic.htm>.
10. Optical Energy Technologies, 2014, http://www.opticalenergytechnologies.com/sun-simulators-solar-simulator
11. "Parabolic Prodcuts." *Manufacturing Electroformed Reflectors, Parabolic Reflectors, Cold Sheilds and Vacuum Coating*. Optiforms, n.d. Web. 06 Apr. 2014. <http://www.optiforms.com/parabolic.htm>.
12. Howell, J.R., "A catalog of radiation configuration factors", McGraw-Hill, 1982.
13. "Ray Tracing." *Computer Science*. University of Utah, n.d. Web. <http://www.cs.utah.edu/~shirley/books/fcg2/rt.pdf>.
14. Narasimhan, Balasubramanian. "The Normal Distribution." *No Title*. N.p., 21 July 1996. Web. 01 Apr. 2014.
15. Siegel, Nathan, Dan Shneyer, Josh McCall, Justin Jones, Ian Rafter, and Jason Scalera. "Design and Evaluation of a Lower Cost, High Flux Solar Simulator." 23 July 2012. Lecture.
16. Urbano, Lensyl. "Parabolic Mirrors." *Montessori Muddle RSS*. N.p., 28 Jan. 2012. Web. 1 Apr. 2014. <http://montessorimuddle.org/2012/01/28/parabolic-mirrors/>.
17. Rabl, Ari. "Comparison of Solar Concentrators." *Solar Energy* 18 (1976): 93-111. Web.

Appendix I: Collimator Calculations

The divergence of light exiting the end of the collimator was a function of the length and diameter of the tubes (Figure I.a). Drinking straws, which have a 7 mm diameter, were used for the analysis. The angular divergence, α, was 9.2 mRadians for the calculations.

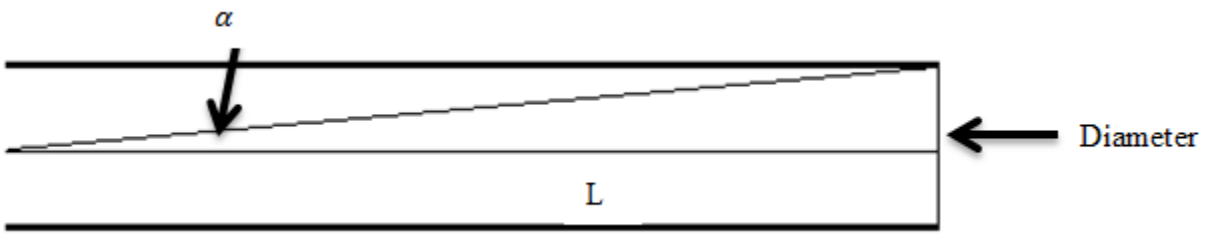

Figure I.a: A model of a tube to demonstrate how the length and the diameter of the tube dictate the angular divergence, α

Since α and the diameter are both known, trigonometry can be used to solve for L with the equation

$$L = \frac{Diameter}{\tan(\alpha)} \tag{I.a}$$

$$L = \frac{0.007\ meters}{\tan(0.0092)} = 0.8\ meters$$

Appendix II: Angular Divergence Derivation

Appendix II.a *Equation derivations*

To determineα, other geometrical properties of the parabolic mirror had to be measured first. The distance between the lamp and the vertex of the parabolic reflector dictates the rim angle, ϕ_{rim} . From the rim angle and the diameter of the aperture, D_{app}, the focal point, f_{fp}, can be found using the equation

$$f_{fp} = \frac{D_{app}}{4\tan\left(\frac{\phi}{2}\right)} \tag{II.1}$$

Finding the x coordinate was dependent on the size of the rim angle, and was calculated with the equations

For $\phi < \frac{\pi}{2}$
$$x_{edge} = f_{fp} - \frac{D_{app}}{2}\frac{1}{\tan\left(\frac{\pi}{2} - \phi\right)} \tag{II.2}$$

For $\phi = \frac{\pi}{2}$
$$x_{edge} = f_{fp} \tag{II.3}$$

For $\phi > \frac{\pi}{2}$
$$x_{edge} = f_{fp} + |\frac{D_{app}}{2}\frac{1}{\tan\left(\frac{\pi}{2} - \phi\right)}| \tag{II.4}$$

The coordinates of the rim's edge can be defined as

$$(x_{edge}, y_{edge}) = (x_{edge}, \ \frac{D_{app}}{2}) \tag{II.5}$$

The focal point location is

$$(x_{fp}, y_{fp}) = (f_{fp}, 0) \tag{II.6}$$

The vector coordinates are then used to determine the length between the two points and is found with the equation

$$\left(L_x, L_y\right) = \left(x_{edge}, y_{edge}\right) - (x_{fp}, y_{fp}) \tag{II.7}$$

The scalar distance between the focal point and the parabolic mirror's edge is found with the equation

$$L = \sqrt{L_x^2 + L_y^2} \tag{II.8}$$

With these values, the maximum angle of divergence, α, is found with the equation

$$\alpha = 2\frac{atan(\frac{d_{source}}{2})}{L} \tag{II.9}$$

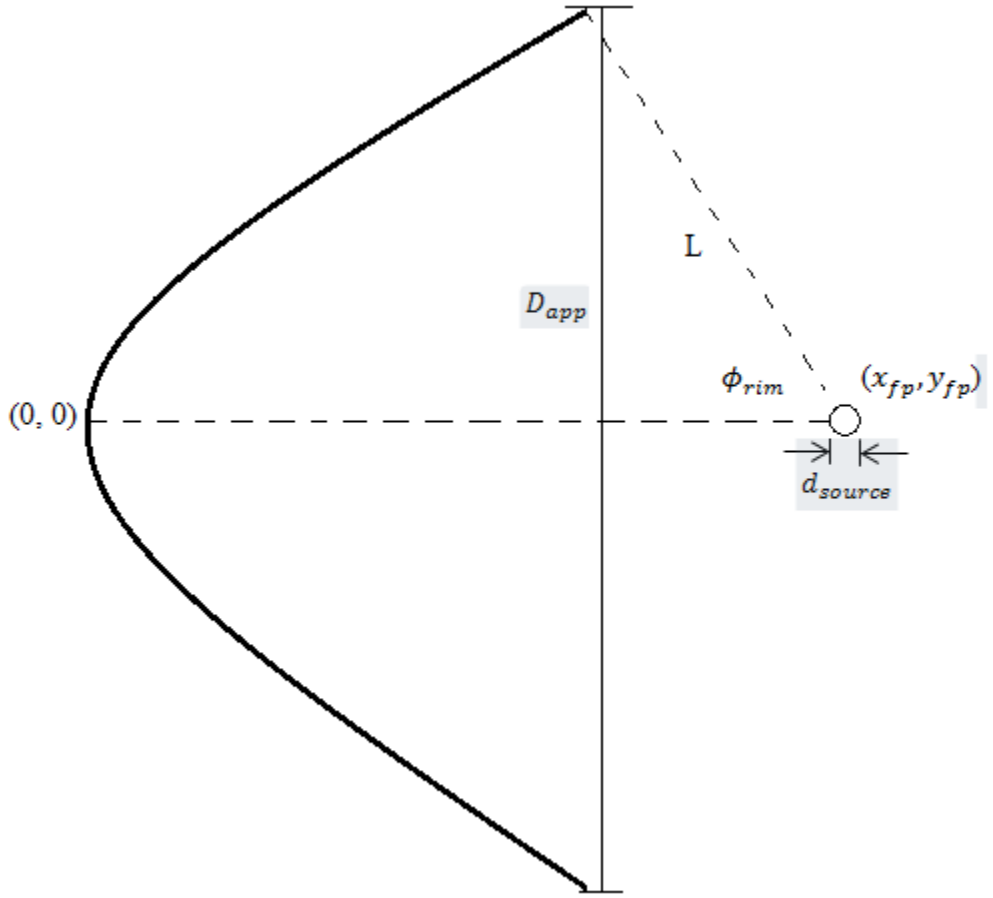

Figure II.a: Variables in a parabolic mirror required to calculate the angular divergence

Appendix II.b: *MATLAB Code for Angular Divergence and Efficiency*

```
close all
clear all

d_app = input('Aperature diameter (m): ');
%d_source = 0.001:0.001:0.025;

d_source = 0.0095;

% Angle of Apperature
phi_15 = pi/12; phi_30 = pi/6; phi_45 = pi/4;
phi_60 = pi/3; phi_90 = pi/2; phi_120 = 2*pi/3; %Radians

%Find the focal length for each corresponding angle
f1 = d_app/(4*tan(phi_15/2)); f2 = d_app/(4*tan(phi_30/2));
f3 = d_app/(4*tan(phi_45/2)); f4 = d_app/(4*tan(phi_60/2));
f5 = d_app/(4*tan(phi_90/2)); f6 = d_app/(4*tan(phi_120/2));

focal = [f1 f2 f3 f4 f5 f6]';
focal_m = [f1, 0; f2, 0;  f3, 0; f4, 0;  f5, 0; f6, 0];


% Coordinate of the edge of parabolic mirror

loc_edge15 = f1 - d_app/2*tan(pi/2 - phi_15);
loc_edge30 = f2 - d_app/2*tan(pi/2 - phi_30);
loc_edge45 = f3 - d_app/2*tan(pi/2 - phi_45);
loc_edge60 = f4 - d_app/2*tan(pi/2 - phi_60);
loc_edge90 = f5;
loc_edge120 = f6 + abs(d_app/2*tan(pi/2 - phi_120));
loc_edge  =  [loc_edge15;  loc_edge30;  loc_edge45;  loc_edge60;  loc_edge90;
loc_edge120];

loc_edge(:, 2) = zeros(6, 1);
loc_edge(:, 2) = d_app/2;
l_foc_edge = loc_edge - focal_m; %vector distance from focal to edge of dish
scalar_l = (sqrt(l_foc_edge(:, 1).^2 + l_foc_edge(:, 2).^2))'; %scalar length
from focal to edge of dish

% angle of deflection
alpha15 = 2.*atan((d_source./2)./scalar_l(1, 1));
alpha30 = 2.*atan((d_source./2)./scalar_l(1, 2));
alpha45 = 2.*atan((d_source./2)./scalar_l(1, 3));
alpha60 = 2.*atan((d_source./2)./scalar_l(1, 4));
alpha90 = 2.*atan((d_source./2)./scalar_l(1, 5));
alpha120 = 2.*atan((d_source./2)./scalar_l(1, 6));

alpha = [alpha15, alpha30, alpha45, alpha60, alpha90, alpha120];


H = focal - loc_edge(:, 1);
```

```
h_square = (H./(0.5*d_app));
if  h_square <= 0
    eff = 1 - 1./2.*(1-1./sqrt(1+1./h_square.^2));
else
    eff = 1./2.*(1-1./sqrt(1+1./h_square.^2));
end
```

Appendix III: p174-100 Technical Drawing

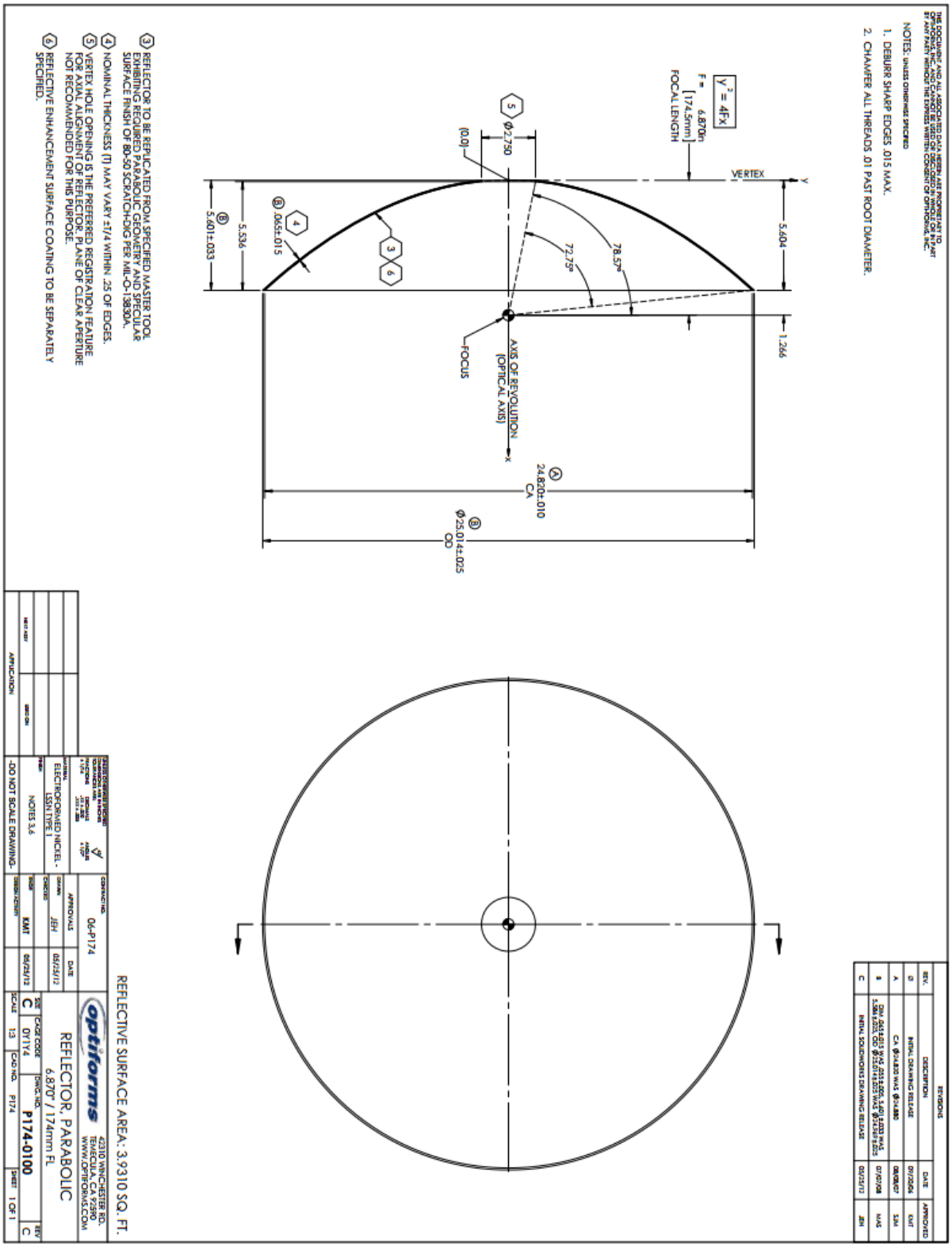

Appendix IV: Spectrum Comparison

The Planck radiation distribution can be used to analyze the spectrum of an object that is approximated as a blackbody and is calculated using the equation

$$E = \frac{2hc^2}{\lambda^5}\frac{1}{e^{\frac{hc}{\lambda kT}} - 1} \tag{IV.1}$$

The constants in this equation can be found in Table IV.1, while the input variables are wavelength, λ, and temperature, T.

Table IV.1: The constants used in the Planck radiation distribution formula

Variable	Name	Value	Units
h	Planck's Constant	6.626×10^{-34}	$\frac{m^2 kg}{s}$
k	Boltzmann's Constant	1.38×10^{-23}	$\frac{m^2 kg}{s^2 K}$
c	Speed of Light	3×10^{8}	$\frac{m}{s}$

The analysis of the solar spectrum used a temperature of 5,800 K, while the input temperature for the lamp was 6,000 K. The spectrum over the range of wavelengths was then averaged using the equation

$$\frac{E_{6000} - E_{5800}}{E_{5800}} = \%\, difference \tag{IV.2}$$